

Synthesis and Biological Evaluation of Xanthone Derivatives as Anti-Cancer Agents Targeting Topoisomerase II and DNA

Yali Song (✉ songyali999999@163.com)

Hebei University

Xinyue Zhu

Hebei University

Kan Yang

Hebei University

Siran Feng

Hebei University

Yiwen Zhang

Hebei University

Jinjiao Dong

Hebei University

Zhenming Liu

Peking University

Xiaoqiang Qiao

Hebei University

Research Article

Keywords: Xanthone derivatives, Topoisomerase II, Selectivity, Anti-cancer activity, Molecular docking

Posted Date: October 29th, 2021

DOI: <https://doi.org/10.21203/rs.3.rs-857564/v1>

License: © ⓘ This work is licensed under a Creative Commons Attribution 4.0 International License.

[Read Full License](#)

Version of Record: A version of this preprint was published at Medicinal Chemistry Research on March 12th, 2022. See the published version at <https://doi.org/10.1007/s00044-022-02862-6>.

Abstract

Topoisomerase is one of the most important targets of anticancer drugs. In order to develop effective and low-toxic topoisomerase inhibitors, a series of xanthone derivatives have been designed and synthesized using the principles of skeleton transition. In vitro growth inhibition experiments of human breast cancer(MCF-7), gastric cancer (MGC-803), and cervical cancer(Hela) cell lines were used to evaluate the compound's anti-tumor cell proliferation activity. Most of the compounds showed anti-tumor growth activity, and also showed low toxicity to human normal cells L929. In the enzyme activity inhibition experiment, compounds 7d and 8d showed the best inhibitory activity. The DNA binding studies disclosed that the most potent compounds **7d** and **8d** can intercalate into DNA, induce apoptosis in MGC-803 cells and arrested at G2/M phase. Molecular docking showed that compounds **7d** and **8d** could bind with topoisomerase II and DNA through hydrogen bonds and π -stacking interactions.

1. Introduction

In recent years, the incidence and mortality of cancer have been on the rise. Traditional anticancer drugs are mainly some cytotoxic chemotherapy drugs, and the representative drugs include DNA alkylation agents (such as nitrogen mustard), metabolic antagonists (such as methotrexate), tubule inhibitors (such as paclitaxel), and topoisomerase II inhibitors (such as etoposide)^[1]. Targeted cancer therapy, in which the drugs are used to specifically block the growth of cancer by interfering with molecular targets and consequently causing less damage to normal cells, has become one of the high potential cancer treatments^[2, 3]. DNA plays a very important role in the cell cycle, and it is an important target for anti-tumor drugs^[4]. Following the clinical success of the DNA-intercalating topo II inhibitors doxorubicin, mitoxantrone, and analogues as anticancer drugs, a great deal of work has been devoted toward other classes of compounds with similar overall topology as topo II inhibitors^[5-7].

Topoisomerase (Topo) was an enzyme that primarily addresses the conformational problems that arise in DNA during recombination, replication, transcription, and repair^[8-10]. It was a dependent enzyme for eukaryotic cell proliferation and survival^[11]. On the basis of their mechanisms, topoisomerases can be classified into two major classes: Topo I and Topo II. Topo I cleaves one single-stranded DNA during each catalytic cycle^[12, 13]. Topo II breaks one double-stranded DNA strand, allowing another segment of duplex DNA to pass through the transient breakage before resealing the broken strand to resolve DNA knots and tangles^[14, 15]. Because tumor cells have the characteristics of rapid proliferation, the content and activity of topoisomerase were significantly higher than that of normal somatic cells^[16]. Therefore, the rapid proliferation of tumor cells can be prevented by inhibiting the activity of topoisomerase, thus killing tumor cells. In recent years, topoisomerase inhibitors have become one of the hot spots in the research and development of antitumor drugs^[17-20].

Xanthenes are a class of oxygen containing heterocyclic compounds with a broad range of biological activities, and they have prominent significance in the field of medicinal chemistry. They have diverse

biological activities including anti-cancer, antimicrobial^[21], antimalarial^[22], anticholinesterase^[23], anticonvulsant^[24] and antioxidant^[25] activities according to their diverse structures. In recent years, the research on the anti-tumor activity of xanthenes has been studied deeply. Reported to date, oxygenated xanthenes synthesized or isolated from natural resources inhibit the proliferation of several cancer cell lines^[26]. Antitumor targets were found to be topoisomerase^[27], P-glycoprotein^[28], PKC^[29] and IKK β ^[30]. In 2016, Chaomei Liu^[20] *et al.* synthesized 3,6-disubstituted methoxy amido xanthene derivatives. The compounds have good anti-tumor activity. They are resistant to MDA-MB-231, PC-3, A549, AsPC-1 and HCT116, the IC₅₀ values of these cells are 8.06, 6.18, 4.59, 4.76, 6.09 μ M, respectively. In 2017, Elirosa Minniti^[31] *et al.* designed and synthesized a series of xanthone derivatives and tested them for TopoIIa inhibitory activity. The results showed that the target compounds have inhibitory effects on TopoIIa, with IC₅₀ values ranging from 1.0 to 2.5 μ M. It can be seen that the xanthone derivatives have good anti-cancer activity targeting Topo II and high development value.

Based on the excellent antitumor activity of xanthenes, we designed and synthesized a series of xanthenes derivatives and studied the effect of different substituents on anticancer activity. The evaluation of biological activities of these compounds was carried out for topoisomerase I and II inhibitory activity, DNA binding activity and cytotoxicity against several human cancer cell lines.

2. Results And Discussion

2.1 Chemistry

i: acetic anhydride, 70 °C, 0.5 h; ii: 2-chloro-5-nitrobenzoic acid, Cu, K₂CO₃, DMF, 130 °C, 8-10h; iii: H₂SO₄, 70 °C, 5 h; iv: chloroacetyl chloride or 3-chloropropionyl chloride, triethylamine, dichloromethane, ice bath, overnight; v: secondary amine, acetonitrile, K₂CO₃, KI, 70 °C, 5 h. vi: ethyl acetate, SnCl₂, HCl, 70 °C, 1 h; vii: secondary amine, acetonitrile, K₂CO₃, KI, 70 °C, 0.5-2 h.

The synthetic route of the target compounds **7a-7g**, **8a-8g**, **11a-11g**, **12a-12f** are described in Scheme 1. 2-(3-aminophenoxy)-5-nitrobenzoic acid **3** was afforded from 3-acetamidophenol and 2-chloro-5-nitrobenzoic acid as raw material via Ullmann reaction, then dehydration provided 6-amino-2-nitro-9H-xanthen-9-one **4**^[32]. The intermediate **4** was reacted with different acyl chloride to obtain the amide analogues **5** and **6** in the dichloromethane solvent system. Compounds **5** or **6** with different secondary amines provided target compounds **7a-7g**, **8a-8g**. Compounds **5** and **6** were reduced to compounds **9** and **10** under the catalysis of stannous chloride. The target analogues **11a-11g** and **12a-12f** were easily obtained at the reflux condition with different secondary amines.

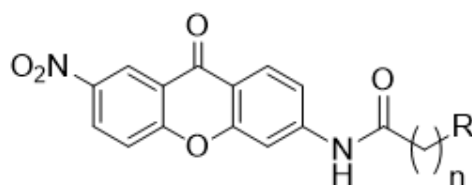
2.2 Antiproliferative activity

All compounds were assessed for *in vitro* anti-proliferative activity using MTT assay against three different human cancer cell lines MCF-7 (human breast cancer), Hela (human cervical cancer), MGC-803 (human gastric cancer), and a normal cell L929 (fibroblasts cell line), etoposide, camptothecine and

adriacin were used as positive controls. The inhibitory activities (IC_{50} values) of the compounds against tested cancer cell lines and a normal cell are listed in Table 1 and Table 2.

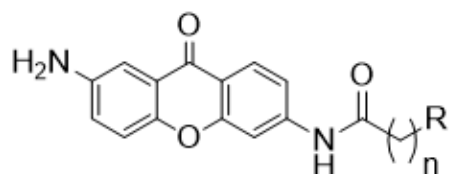
As shown in Table 1 and Table 2, all of the target compounds had the best inhibitory effect on MGC-803, and poor effect on HeLa. Among them, compounds **7d**, **8a**, **8c**, **8d**, **8e**, **8f**, **8g** and **12c** showed well anti-proliferation against MGC-803 cancer cell lines with IC_{50} values lower than 10 μ M. In general, most of the compounds showed better activity when n is 2 than when n is 1. When R is substituted by the same secondary amines, the nitro-substituted compounds on the xanthone ring are more cytotoxic than amino-substituted compounds.

Table 1. Antiproliferative activity of compounds **7a-7g**, **8a-8g** against cancer and normal cell line.



comp	n	R	IC_{50} (μ M)			
			HeLa	MGC-803	MCF-7	L929
7a	1	diethylamine	>80	19.2 \pm 1.28	>80	98.37 \pm 6.06
7b	1	morpholine	>80	20.12 \pm 0.56	52.02 \pm 0.15	47.00 \pm 3.46
7c	1	pyrrolidine	>80	68.2 \pm 3.46	>80	60.67 \pm 4.28
7d	1	N-methylpiperazine	19.81 \pm 1.36	10.06 \pm 0.89	18.09 \pm 1.15	9.458 \pm 1.16
7e	1	N-ethyl piperazine	42.02 \pm 3.15	20.21 \pm 1.45	34.99 \pm 0.55	7.888 \pm 0.83
7f	1	2-methylpiperidine	>80	>80	>80	77.82 \pm 5.83
7g	1	piperidine	>80	>80	35.35 \pm 2.56	51.78 \pm 5.16
8a	2	diethylamine	11.04 \pm 0.56	7.188 \pm 0.26	6.994 \pm 0.45	15.44 \pm 0.86
8b	2	morpholine	>80	22.34 \pm 1.46	57.81 \pm 4.50	136.7 \pm 6.42
8c	2	pyrrolidine	16.24 \pm 1.23	6.672 \pm 0.65	7.66 \pm 0.56	13.96 \pm 1.96
8d	2	N-methyl piperazine	22.65 \pm 1.23	8.03 \pm 0.45	6.969 \pm 0.62	13.52 \pm 2.18
8e	2	N-ethyl piperazine	36.64 \pm 2.56	10.53 \pm 1.24	20.38 \pm 1.73	44.28 \pm 5.46
8f	2	2-methyl piperidine	8.904 \pm 0.26	7.382 \pm 0.45	6.597 \pm 0.86	17.41 \pm 1.34
8g	2	piperidine	40.98 \pm 5.23	9.24 \pm 1.35	7.073 \pm 1.53	31.09 \pm 3.45
Etoposide	-	-	5.35 \pm 0.56	18.3 \pm 1.28	4.918 \pm 0.56	80.36 \pm 5.92
Adriacin	-	-	0.032 \pm 0.15	0.085 \pm 0.35	0.045 \pm 0.28	100 \pm 7.15
Camptothecine	-	-	0.07 \pm 0.43	0.029 \pm 0.25	1.07 \pm 0.43	58.47 \pm 0.73

Table 2. Antiproliferative activity of compounds **11a-11g**, **12a-12f** against cancer and normal cell.



comp	n	R	IC ₅₀ (μM)			
			Hela	MGC-803	MCF-7	L929
11a	1	diethylamine	>80	>80	>80	151.3±6.45
11b	1	morpholine	>80	>80	>80	170.0±9.15
11c	1	pyrrolidine	48.08±2.83	32.54±2.48	53.14±3.18	48.34±2.56
11d	1	N-methyl piperazine	55.85±3.18	16.81±1.86	26.08±2.05	69.81±5.15
11e	1	N-ethyl piperazine	36.81±1.59	15.09±1.82	23.1±1.94	34.69±2.56
11f	1	2-methyl piperidine	>80	49.42±2.59	>80	73.89±3.82
11g	1	piperidine	>80	>80	>80	96.07±2.18
12a	2	Diethylamine	>80	19.19±1.29	35.35±1.39	48.32±1.81
12b	2	morpholine	>80	34.63±1.59	>80	60.22±2.58
12c	2	pyrrolidine	57.11	6.311±1.82	8.818±0.82	11.36±1.56
12d	2	N-methyl piperazine	>80	31.74±1.98	54.85±2.85	61.57±3.81
12e	2	N-ethyl piperazine	>80	14.82±1.05	43.8±2.46	43.88±1.56
12f	2	2-methyl piperidine	>80	23.98±1.82	39.55±1.95	37.29±1.48
Etoposide	-	-	5.35±0.65	18.30±1.26	4.918±0.95	80.36±2.53
Adriacin	-	-	0.032±0.48	0.085±0.32	0.045±0.15	100±3.15
Camptothecine	-	-	0.07±0.43	0.029±0.25	1.07±0.43	58.47±0.73

2.3 DNA topoisomerase I inhibition activity

The inhibitory properties of the compounds against topoisomerase I was determined by DNA relaxation assay using agarose gel electrophoresis^[33]. Camptothecin as a potent Topoisomerase I inhibitor, was used as positive control in this test. The obtained results of topoisomerase I inhibitory properties of the compounds were presented in Fig. 1. As shown in Fig. 1, in the blank control group (Lane D), DNA kept the supercoil structure during electrophoresis and ran the farthest. In the negative control group (Lane T), DNA was completely transformed from supercoiled DNA to relaxed DNA under the action of Topo I. In the experimental group (Lane C and Lanes **7a-7g**, **8a-8g**, **11a-11g** and **12a-12f**), the positive control camptothecin can almost completely inhibit the relaxation effect mediated by Topo I, and DNA still maintains a supercoiled structure (Line C). While none of the tested compounds **7a-7g**, **8a-8g**, **11a-11g**

and **12a-12f** exhibited topoisomerase I inhibition potency even at 100 μM , indicating that these compounds may display selective inhibition against Topoisomerase II.

2.4 DNA topoisomerase II inhibitory activity

All compounds were evaluated the inhibitory activities against topoisomerase II by pBR322 DNA relaxation assay at a high concentration of 100 μM for the screening of candidate topoisomerase inhibitors^[34]. Etoposide was used as positive control for topoisomerase II. The obtained results of topoisomerase II inhibitory properties of the compounds were presented in Fig. 2. As shown in Fig. 2, most of the compounds (**7a**, **7b**, **7d**, **7e**, **7g**, **8a**, **8b**, **8d**, **8e**, and **8g**) exhibit inhibitory activity. Among them, compounds **7d** and **8d** with N-methylpiperazine showed significant inhibitory activity at 20 μM . As shown in Fig. 2, 11a-11g and 12a-12f with amino substitution groups on xanthone ring showed none inhibitory. None of the tested compounds exhibited topoisomerase I inhibition potency, and most of the compounds showed selective inhibition for topoisomerase II.

2.5. UV-Visible titration assay

UV-Visible studies are useful in examining the mode of binding of DNA with small molecules^[35, 36]. When small molecules intercalated into DNA, the stacking interaction between aromatic chromophore and the base pairs of DNA will lead to bathochromic shifts and hypochromicity on the UV-Visible curve of compound-DNA complex^[37, 38]. In the absence of ctDNA, all the compounds has absorption peak at around 300 nm. Increasing ctDNA concentration, the absorption bands of **7d**, **7e**, **8d**, and **8e** displayed clear hypochromism with a concomitant minor red shift. The results indicated that **7d**, **7e**, **8d**, and **8e** probably interact with DNA by intercalation mode, involving a stacking interaction between xanthone ring of compounds and DNA base pairs.

2.6 EB displacement assay

The intercalation mode of compounds binding to DNA was further examined using the competitive binding ethidium bromide (EB) displacement assay^[3]. The DNA bound form of EB has a stronger fluorescence emission than free EB. If there is a compound compete with EB for DNA-binding sites, the fluorescence quenching of DNA-EB system is observed, so the DNA-EB displacement experiments could be investigated whether compounds can intercalate into DNA^[39]. As showed in Fig. 4, the emission intensity of DNA-EB system at about 600 nm decreased distinctly when the concentration of **7d**, **7e**, **8d**, and **8e** increased, indicating that these compounds can intercalate into DNA.

2.7 DNA unwinding assay

The unwinding effect is caused by certain compounds intercalating into the DNA, and the effect may yield false positive outcomes in the Topo-mediated DNA relaxation assay^[40]. In order to determine the intercalating or non-intercalating ability of these compounds, a DNA unwinding assay was carried out using supercoiled pBR322 DNA as substrate and EB as control^[3, 8]. As shown in Fig. 5, EB, a classic DNA

intercalator, is able to transform the relaxed DNA into supercoiled DNA in the presence of excess Topoisomerase in a dose dependent manner. And compounds **7d**, **7e**, **8d** and **8e** could intercalate into DNA at 200 μM . This finding provides evidence that these compounds were DNA intercalator.

2.8 Annexin V-FITC/PI (AV/PI) dual staining assay

According to the above experiments, compounds **7d** and **8d** could inhibit the activity of Topo II and interact with DNA, which may induce apoptosis in cancer cell lines. Annexin V and PI dual staining assay was used to detect early and late apoptotic cells (annexin-V⁺/PI⁻ and annexin-V⁺/PI⁺), necrotic (annexin-V⁻/PI⁺) as well as viable cells (annexin-V⁻/PI⁻)^[41]. As showed in Fig. 6, **7d** as well as **8d** significantly increased the percentage of late apoptotic cells in comparison with untreated cells. After 48 h of incubation, a significant proapoptotic effect was observed in MGC-803 in all cases. At a concentration of 2.5 μM , the late apoptotic rates of compound **7d** and **8d** on MGC-803 cells were 6.53% and 10.59%, respectively. When the concentration was increased to 10 μM , the late apoptotic rates of compound **7d** and **8d** on MGC-803 cells increased to 91.20%, 98.13% respectively.. It can be seen that the compound can significantly inhibit the late apoptosis of MGC-803 cells, and the inhibitory rate of compound **8d** on the late apoptosis of cells is greater than that of **7d**, which further proves that the carbon chain of the substituent at position 6 of the compound When the length is longer, the inhibitory effect on cancer cells is greater.

2.9 Cell cycle analysis

The cell cycle analysis experiment^[42] used different concentrations of compounds **7d** and **8d** (2.5, 5 μM) to treat MGC-803 cells to detect which stage of the growth cycle the cells were blocked. The experimental results showed that after 48h of compounds treatment, the cell population in G2/M phase increases from 2.51% in the untreated cells to 4.76% and 9.19% in the cells treated with **7d** at 2.5, 5 μM , and from 2.51% in the untreated cells to 6.86% and 15.45% in the cells treated with **8d**, respectively. Obviously, these compounds arrested cell growth in the G2/M phase and caused cell apoptosis.

Table 3. Effect of compounds **7d and **7f** on cell cycle phase distribution in MGC-803 cells.**

Compounds	G0/G1	S	G2/M
A: Control	50.58	46.91	2.51
B: 7d (2.5 μM)	51.72	43.52	4.76
C: 7d (5 μM)	46.03	44.78	9.19
D: 8d (2.5 μM)	52.92	40.22	6.86
E: 8d (5 μM)	43.00	41.56	15.45

2.10 Molecular docking

Compounds **7d** and **8d** exhibited Topo II inhibition and efficient DNA binding abilities. In order to visualize the binding mode of the title compounds, molecular docking studies were performed with human

topoisomerase II (PDB ID: 4G0V) and DNA (PDB ID: 2DES).

These compounds fit well into mitoxantrone binding pocket present in DNA-Topo II, complex xanthone ring intercalated with DNA and one benzene ring of xanthone exhibited π -stacking interactions with ARG503 residues, DG13 nitrogen bases and another benzene ring of xanthone exhibited π -stacking interactions with DA12 and DG13 nitrogen bases (Fig. 6A and B). Additionally, the carbonyl group in **7d** of xanthone ring form hydrogen-bonding with the side chain of GLN778 and DT9 (Fig. 6A) and the carbonyl group in **8d** of xanthone ring form hydrogen-bonding with the side chain of GLN778 (Fig. 6B). N atoms on the piperazine ring on the side chain form hydrogen bonds with DC11.

The molecular docking studies revealed that the xanthone ring is responsible for intercalation, and xanthone ring substituents exhibited π -stacking interactions with DG8 and DG6, nitrogen and nitro form metal bonds with Mg^{2+} (Fig. 6C and D).

3. Conclusions

Xanthone derivatives are co-planar structures obtained by the fusion of multiple aromatic rings, and this is the key for them to enter the topoisomerase activity pocket, where the substituents on the amino nitrogen have a greater impact on the anti-tumor activity. Among these compounds, **7d** and **8d** with N-methyl piperazine substituent showed excellent anti-tumor cell proliferation activity and topo II inhibitory activity. DNA binding studies disclosed that **7d** and **8d** were DNA intercalator, and this is correlated with the docking studies. Annexin V-FITC/PI assay revealed that these compounds induce apoptosis in MGC-803. Cell cycle analysis indicated that these compounds stop the cell cycle at G2/M phase.

4. Experimental

4.1 Chemistry

4.1.1 General

Most chemicals and reagents were obtained commercially of analytical grade and used without further purification. Reactions were monitored by thin-layer chromatography (TLC) using precoated silica gel plates (silica gel GF/UV 254), and spots were visualized under UV light (254 nm).

1H NMR and ^{13}C NMR are measured on a Bruker AVANCE III 600MHz (Switzerland) spectrometer in $DMSO-d_6$, using TMS as the internal standard. High Resolution Mass Spectral (HRMS) data is determined on a Thermo Fisher Scientific Q Exactive mass spectrometer.

4.1.2. Synthesis of intermediates

Compounds **2**, **3**, **4**, **5**, **6** were prepared according to the reported^[43]. Compounds **5** or **6** and $SnCl_2$ dissolved in acetic ether, then hydrochloric acid was added. The mixture was stirred well for 6 h at $70^\circ C$

and monitored by TLC. After cooling to room temperature, the reaction mixture was poured over a saturated solution of NaHCO₃. Light yellow precipitate appeared was collected by filtration and crystallized to produce compound **9** or **10**.

To a stirred refluxing suspension of compounds **5** (or **6**, **9**, **10**) (1 mmol), K₂CO₃ (2mmol) and KI (0.6 mmol) in acetonitrile (10 mL) was added dropwise appropriate secondary amine (1.0 mL) which dissolved in acetonitrile (10 mL). The mixture was stirred under reflux for 6 h, cooled down to room temperature, and diluted with distilled water. The precipitate was filtered, washed with ether, dried and evaporated to afford raw product, and further recrystallized by acetone and hydrochloride acid to yield **7a-7g** (or **8a-8g**, **11a-11g**, and **12a-12f**).

2-(diethylamino)-N-(7-nitro-9-oxo-9H-xanthen-3-yl)acetamide (**7a**), White solid, 32.5% yield. ¹H NMR (600 MHz, DMSO-d₆) δ 9.76 (s, 1H, -NH-), 8.87 (d, J = 2.8 Hz, 1H, -ArH), 8.63 (dd, J = 9.2, 2.8 Hz, 1H, -ArH), 8.24 (d, J = 8.7 Hz, 1H, -ArH), 8.14, (d, J = 1.7 Hz, 1H, -ArH), 7.93 (d, J = 9.2 Hz, 1H, -ArH), 7.66 (dd, J = 8.7, 1.7 Hz, 1H, -ArH), 3.33 (s, 2H, -COCH₂), 2.10–2.08 (m, 4H, -CH₂), 1.26 (t, J = 7.2 Hz, 6H, -CH₃). ¹³C NMR (151 MHz, DMSO) δ 177.7, 166.1, 158.1, 156.1, 143.3, 140.1, 134.2, 127.1, 121.8, 120.2, 119.8, 118.3, 108.9, 81.5, 53.1, 48.6, 8.9. HRMS (ESI⁺) [M + H]⁺C₁₉H₂₀N₃O₅: 370.1403, Found: 370.1373.

2-morpholino-N-(7-nitro-9-oxo-9H-xanthen-3-yl)acetamide (**7b**), White solid, 27.5% yield. ¹H NMR (600 MHz, DMSO-d₆) δ 11.90 (s, 1H, -NH-), 8.80 (d, J = 2.8 Hz, 1H, -ArH), 8.59 (dd, J = 9.2, 2.8 Hz, 1H, -ArH), 8.17 (d, J = 8.7 Hz, 1H, -ArH), 8.11 (d, J = 1.6 Hz, 1H, -ArH), 7.88 (d, J = 9.2 Hz, 1H, -ArH), 7.68 (dd, J = 8.7, 1.6 Hz, 1H, -ArH), 4.38 (s, 2H, -COCH₂), 3.98–3.71 (m, 4H, -OCH₂), 3.38–2.95 (m, 4H, -NCH₂). ¹³C NMR (151 MHz, DMSO-d₆) δ 173.8, 158.7, 156.0, 155.9, 144.6, 143.3, 129.1, 127.1, 121.7, 121.0, 120.1, 116.6, 106.6, 99.3, 62.9, 56.4, 51.7. HRMS (ESI⁺) [M + H]⁺C₁₉H₁₈N₃O₅: 383.1117, Found: 382.1369.

N-(7-nitro-9-oxo-9H-xanthen-3-yl)-2-(pyrrolidin-1-yl)acetamide(**7c**), White solid, 26.9% yield. ¹H NMR (600 MHz, DMSO-d₆) δ 11.71 (s, 1H, H⁺), 10.43 (s, 1H, -NH-), 8.82 (d, J = 2.8 Hz, 1H, Ar-H), 8.61 (dd, J = 9.2, 2.8 Hz, 1H, Ar-H), 8.18 (d, J = 8.7 Hz, 1H, Ar-H), 8.11 (d, J = 1.2 Hz, 1H, Ar-H), 7.89 (d, J = 9.2 Hz, 1H, Ar-H), 7.66 (dd, J = 8.7, 1.2 Hz, 1H, Ar-H), 4.41 (s, 2H, -COCH₂), 2.52–2.50 (m, 4H, -CH₂), 2.08–1.93 (m, 4H, -CH₂). ¹³C NMR (151 MHz, DMSO-d₆) δ 174.1, 170.7, 158.8, 156.32, 145.1, 143.5, 129.2, 127.4, 121.9, 121.3, 120.3, 116.7, 116.6, 106.9, 61.8, 55.9, 22.8. (ESI⁺) [M + H]⁺ C₁₉H₁₈N₃O₅: 368.1246, Found: 368.1223.

2-(4-methylpiperazin-1-yl)-N-(7-nitro-9-oxo-9H-xanthen-3-yl)acetamide (**7d**), White solid, 25.7% yield. ¹H NMR (600 MHz, DMSO-d₆) δ 10.39 (s, 1H, -NH-), 8.84 (d, J = 2.8 Hz, 1H, Ar-H), 8.61 (dd, J = 9.2, 2.8 Hz, 1H, Ar-H), 8.20 (d, J = 1.8 Hz, 1H, Ar-H), 8.15 (d, J = 8.7 Hz, 1H, Ar-H), 7.90 (d, J = 9.2 Hz, 1H, Ar-H), 7.63 (dd, J = 8.7, 1.8 Hz, 1H, Ar-H), 3.22 (s, 2H, -COCH₂), 3.18–3.17 (m, 4H, -CH₂), 3.17–3.16 (m, 4H, -CH₂), 2.18 (s, 3H, -CH₃). ¹³C NMR (151 MHz, DMSO-d₆) δ 173.8, 169.6, 158.9, 156.3, 145.5, 143.4, 129.1, 126.9, 121.8, 121.2, 120.2, 116.8, 116.0, 106.2, 61.8, 54.5, 52.6, 45.7. HRMS (ESI⁺) [M + H]⁺ C₂₀H₂₁N₄O₅: 397.1512 Found: 397.1482

N-2-(4-ethylpiperazin-1-yl)-N-(7-nitro-9-oxo-9H-xanthen-3-yl)acetamide (**7e**), White solid, 63.0% yield. ^1H NMR (600 MHz, DMSO- d_6) δ 10.39 (s, 1H, -NH-), 8.83 (s, 1H, Ar-H), 8.60 (d, J = 7.8 Hz, 1H, Ar-H), 8.19 (s, 1H, Ar-H), 8.13 (d, J = 8.4 Hz, 1H, Ar-H), 7.89 (d, J = 8.4 Hz, 1H, Ar-H), 7.62 (d, J = 7.8 Hz, 1H, Ar-H), 3.31 (s, 2H, -COCH $_2$), 2.50–2.43 (m, 8H, -CH $_2$), 2.34–2.33 (m, 2H, -CH $_2$), 1.00 (t, J = 6.0 Hz, 3H, -CH $_3$). ^{13}C NMR (151 MHz, DMSO- d_6) δ 173.9, 169.7, 158.9, 156.3, 145.6, 143.4, 129.1, 127.0, 121.9, 121.2, 120.2, 116.8, 116.1, 106.2, 61.9, 52.8, 52.1, 51.6, 11.9. HRMS (ESI $^+$) $[\text{M} + \text{H}]^+$ C $_{21}\text{H}_{23}\text{N}_4\text{O}_5$: 411.1668, Found: 411.1636.

2-(2-methylpiperidin-1-yl)-N-(7-nitro-9-oxo-9H-xanthen-3-yl)acetamide(**7f**), White solid, 33.3% yield. ^1H NMR (600 MHz, DMSO- d_6) δ 10.33 (s, 1H, -NH-), 8.87 (d, J = 2.6 Hz, 1H, Ar-H), 8.64 (dd, J = 9.2, 2.6 Hz, 1H, Ar-H), 8.23 (d, J = 8.7 Hz, 1H, Ar-H), 8.17 (s, 1H, Ar-H), 7.94 (d, J = 9.2 Hz, 1H, Ar-H), 7.75 (d, J = 8.7 Hz, 1H, Ar-H), 3.32 (s, 2H -COCH $_2$), 2.09 (s, 2H, -CH $_2$), 1.97–1.64 (m, 6H, -CH $_2$), 1.50 (s, 1H, -CH), 1.36 (d, J = 6.3 Hz, 3H, -CH $_3$). ^{13}C NMR (151 MHz, DMSO- d_6) δ 174.1, 170.3, 158.8, 155.6, 145.5, 144.1, 129.4, 127.3, 121.9, 121.2, 120.1, 116.8, 116.2, 106.5, 66.1, 61.7, 53.5, 33.5, 27.2, 25.4, 20.8. HRMS (ESI $^+$) $[\text{M} + \text{H}]^+$ C $_{21}\text{H}_{22}\text{N}_3\text{O}_5$:396.1559, Found: 396.1526.

N-(7-nitro-9-oxo-9H-xanthen-3-yl)-2-(piperidin-1-yl)acetamide (**7g**), White solid, 33.3% yield. ^1H NMR (600 MHz, DMSO- d_6) δ 11.84 (s, 1H, H $^+$), 10.05 (s, 1H, -NH-), 8.84 (d, J = 2.7 Hz, 1H, -Ar-H), 8.62 (dd, J = 9.2, 2.8 Hz, 1H, -Ar-H), 8.20 (d, J = 8.7 Hz, 1H, -Ar-H), 8.14 (d, J = 1.8 Hz, 1H, -Ar-H), 7.91 (d, J = 9.2 Hz, 1H, -Ar-H), 7.69 (dd, J = 8.7, 1.8 Hz, 1H, -Ar-H), 3.13 (s, 2H, -COCH $_2$), 2.52–2.50 (m, 4H, -CH $_2$), 1.90–1.68 (m, 6H, -CH $_2$). ^{13}C NMR (151 MHz, DMSO- d_6) δ 174.0, 169.8, 158.9, 156.3, 144.9, 143.5, 129.3, 127.4, 121.9, 121.2, 120.3, 116.7, 116.5, 106.7, 57.3, 53.1, 22.2, 21.0. HRMS (ESI $^+$) $[\text{M} + \text{H}]^+$ C $_{20}\text{H}_{20}\text{N}_3\text{O}_5$: 382.1403, Found: 382.1368.

3-(diethylamino)-N-(7-nitro-9-oxo-9H-xanthen-3-yl)propanamide(**8a**), White solid, 48.4% yield, ^1H NMR (600 MHz, DMSO- d_6) δ 10.59 (s, 1H, -NH-), 8.85 (t, J = 2.7 Hz, 1H, -ArH), 8.62 (dd, J = 9.2, 2.6 Hz, 1H, -ArH), 8.20–8.15 (m, 2H, -ArH), 7.93 (d, J = 9.2 Hz, 1H, -ArH), 7.68 (dd, J = 8.7, 1.7 Hz, 1H, -ArH), 3.39 (q, J = 6.6 Hz, 2H, -CH $_2$), 3.17–3.13 (m, 4H, -CH $_2$), 3.07 (t, J = 7.4 Hz, 2H, -COCH $_2$), 1.26 (t, J = 7.2 Hz, 6H, -CH $_3$). ^{13}C NMR (151 MHz, DMSO- d_6) δ 173.9, 172.3, 159.0, 156.4, 145.9, 143.4, 129.2, 127.2, 121.9, 121.2, 120.2, 116.6, 116.1, 106.1, 54.9, 46.5, 30.9, 8.4. HRMS (ESI $^+$) $[\text{M} + \text{H}]^+$ C $_{20}\text{H}_{22}\text{N}_3\text{O}_5$:384.1559, Found: 384.1524.

3-morpholino-N-(7-nitro-9-oxo-9H-xanthen-3-yl)propanamide (**8b**), White solid, 9.2% yield. ^1H NMR (600 MHz, DMSO- d_6) δ 11.26 (s, 1H, -NH-), 8.86(d, J = 2.5 Hz, 1H, -ArH), 8.63 (dd, J = 9.2, 2.8 Hz, 1H, -ArH), 8.18–8.17 (m, 2H, -ArH), 7.93 (d, J = 9.2 Hz, 1H, -ArH), 7.64 (d, J = 8.6 Hz, 1H, -ArH), 3.97 (t, J = 5.4 Hz, 4H, -OCH $_2$), 3.78 (t, J = 4.9 Hz, 2H, -CH $_2$), 3.14–3.10 (m, 2H, -COCH $_2$), 3.08 (s, 4H, -NCH $_2$). ^{13}C NMR (151 MHz, DMSO- d_6) δ 174.0, 171.4, 159.0, 156.8, 145.3, 143.5, 128.5, 127.4, 121.9, 121.3, 120.3, 116.7, 116.2, 106.2, 63.3, 54.8, 51.3, 33.4. HRMS (ESI $^+$) $[\text{M} + \text{H}]^+$ C $_{20}\text{H}_{20}\text{N}_3\text{O}_6$: 398.1352, Found: 398.1331.

N-(7-nitro-9-oxo-9H-xanthen-3-yl)-3-(pyrrolidin-1-yl)propanamide (**8c**), White solid, 46.7% yield. ^1H NMR (600 MHz, DMSO- d_6) δ 10.25 (s, 1H, -NH-), 8.85 (d, J = 2.7 Hz, 1H, -ArH), 8.62 (dd, J = 9.2, 2.7 Hz, 1H, -ArH),

8.18 (d, J = 8.7 Hz, 1H, -ArH), 7.94–7.90 (m, 2H, -ArH), 7.59 (d, J = 8.7 Hz, 1H, -ArH), 3.12 (t, J = 7.2 Hz, 2H, -CH₂), 3.00 (t, J = 7.2 Hz, 2H, -COCH₂), 2.03–1.99 (m, 4H, -CH₂), 1.93–1.85 (m, 4H, -CH₂). ¹³C NMR (151 MHz, DMSO-d₆) δ 174.0, 171.9, 159.0, 156.4, 145.7, 143.8, 129.2, 127.2, 121.9, 121.3, 120.3, 116.6, 116.2, 106.2, 53.7, 53.2, 32.4, 22.7. HRMS (ESI⁺) [M + H]⁺ C₂₀H₂₀N₃O₅: 382.1403, Found: 382.1367.

3-(4-methylpiperazin-1-yl)-N-(7-nitro-9-oxo-9H-xanthen-3-yl)propanamide (**8d**), White solid, 64.7% yield. ¹H NMR (600 MHz, DMSO-d₆) δ 12.26 (s, 1H, -NH-), 8.86 (s, 1H, -ArH), 8.65 (d, J = 11.4 Hz, 1H, -ArH), 8.52 (s, 1H, -ArH), 7.91 (d, J = 4.2 Hz, 2H, -ArH), 7.41 (s, 1H, -ArH), 3.67 (s, 2H, -CH₂), 3.25–3.07 (m, 8H, -CH₂), 2.84 (s, 3H, -CH₃), 2.50 (s, 2H, -COCH₂). ¹³C NMR (151 MHz, DMSO-d₆) δ 174.2, 170.3, 158.1, 156.2, 146.3, 143.6, 129.2, 127.1, 121.9, 120.9, 120.1, 116.8, 116.3, 106.3, 57.4, 57.3, 56.2, 53.2, 35.0. HRMS (ESI⁺) [M + H]⁺ C₂₁H₂₃N₄O₅: 411.1668, Found: 411.1631.

3-(4-ethylpiperazin-1-yl)-N-(7-nitro-9-oxo-9H-xanthen-3-yl)propanamide (**8e**), White solid, 8.2% yield. ¹H NMR (600 MHz, DMSO-d₆) δ 10.93 (s, 1H, -NH-), 8.85 (s, 1H, Ar-H), 8.61 (d, J = 9.6 Hz, 1H, Ar-H), 8.17 (s, 1H, Ar-H), 8.14 (d, J = 8.9 Hz, 1H, Ar-H), 7.90 (d, J = 9.4 Hz, 1H, Ar-H), 7.52 (d, J = 8.7 Hz, 1H, Ar-H), 2.66 (s, 2H, -COCH₂), 2.58 (d, J = 5.1 Hz, 2H, -CH₂), 2.49–2.31 (m, 8H, -CH₂), 2.31–2.26 (m, 2H, -CH₂), 0.97 (t, J = 6.6 Hz, 3H, -CH₃). ¹³C NMR (151 MHz, DMSO-d₆) δ 174.9, 170.0, 159.2, 156.8, 146.1, 143.8, 129.7, 127.6, 122.2, 121.4, 120.5, 117.1, 116.4, 106.6, 53.9, 51.9, 51.5, 51.1, 49.0, 47.5, 32.5, 9.3. HRMS (ESI⁺) [M + H]⁺ C₂₂H₂₅N₄O₅: 425.1825, Found: 425.1791.

3-(2-methylpiperidin-1-yl)-N-(7-nitro-9-oxo-9H-xanthen-3-yl)propanamide (**8f**), White solid, 7.5% yield. ¹H NMR (600 MHz, DMSO-d₆) δ 10.80 (s, 1H, -NH-), 8.85 (s, 1H, -ArH), 8.61 (d, J = 9.0 Hz, 1H, -ArH), 8.29–8.02 (m, 2H, -ArH), 7.91 (d, J = 9.1 Hz, 1H, -ArH), 7.49 (d, J = 8.3 Hz, 1H, -ArH), 2.99 (dt, J = 13.5, 6.9 Hz, 2H, -COCH₂), 2.74–2.55 (m, 2H, -CH₂), 2.35 (d, J = 35.5 Hz, 2H, -CH₂), 2.17 (t, J = 10.1 Hz, 1H, -CH-), 1.54 (dt, J = 68.0, 36.0 Hz, 4H, -CH₂), 1.30–1.13 (m, 2H, -CH₂), 1.03 (d, J = 6.0 Hz, 3H, -CH₃). ¹³C NMR (151 MHz, DMSO-d₆) δ 173.7, 171.8, 158.8, 156.3, 146.0, 143.3, 129.0, 127.0, 121.8, 121.1, 120.1, 116.3, 115.7, 105.7, 54.8, 51.5, 49.4, 34.1, 33.2, 25.7, 23.5, 18.6. HRMS (ESI⁺) [M + H]⁺ C₂₂H₂₄N₃O₅: 410.1779, Found: 410.1691.

N-(7-nitro-9-oxo-9H-xanthen-3-yl)-3-(piperidin-1-yl)propanamide (**8g**), White solid, 14.6% yield. ¹H NMR (600 MHz, DMSO-d₆) δ 10.00 (s, 1H, -NH-), 8.85 (d, J = 2.7 Hz, 1H, -ArH), 8.63 (dd, J = 9.2, 2.7 Hz, 1H, -ArH), 8.21 (d, J = 8.7 Hz, 1H, -ArH), 8.14 (s, 1H, -ArH), 7.92 (d, J = 9.2 Hz, 1H, -ArH), 7.68 (dd, J = 8.7, 1.2 Hz, 1H, -ArH), 4.27 (s, 2H, -COCH₂), 3.20–3.01 (m, 2H, -CH₂), 2.54 (s, 4H, -CH₂), 1.83–1.39 (m, 6H, -CH₂). ¹³C NMR (151 MHz, DMSO-d₆) δ 174.0, 158.4, 156.2, 144.6, 143.4, 129.0, 127.7, 121.5, 121.1, 120.5, 116.8, 106.2, 56.7, 55.6, 52.9, 21.9, 20.7. HRMS (ESI⁺) [M + H]⁺ C₂₁H₂₂N₃O₅: 396.1559, Found: 396.1523.

N-(7-amino-9-oxo-9H-xanthen-3-yl)-2-(diethylamino)acetamide (**11a**), Yellow solid, 11.6% yield. ¹H NMR (600 MHz, DMSO-d₆) δ 10.94 (s, 1H, -NH-), 8.14 (d, J = 8.7 Hz, 1H, Ar-H), 8.01 (s, 1H, Ar-H), 7.47 (d, J = 8.6 Hz, 1H, Ar-H), 7.40 (d, J = 8.8 Hz, 1H, Ar-H), 7.26 (d, J = 2.5 Hz, 1H, Ar-H), 7.13 (dd, J = 8.9, 2.6 Hz, 1H, Ar-H),

5.44 (s, 2H, -NH₂), 4.09 (s, 2H, -COCH₂), 3.17 (s, 4H, -CH₂), 1.20 (d, J = 16.7 Hz, 6H, -CH₃). ¹³C NMR (151 MHz, DMSO-d₆) δ 175.0, 162.2, 156.2, 147.8, 145.7, 143.3, 127.1, 122.9, 121.8, 118.5, 116.7, 115.3, 106.4, 106.2, 63.2, 48.5, 11.0. HRMS (ESI⁺) [M + H]⁺ C₁₉H₂₂N₃O₃: 340.1661, Found: 340.1639 .

N-(7-amino-9-oxo-9H-xanthen-3-yl)-2-morpholinoacetamide (**11b**) Yellow solid, 8.4% yield, ¹H NMR (600 MHz, DMSO-d₆) δ 10.27 (s, 1H, -NH-), 8.15 (d, J = 8.7 Hz, 1H, -ArH), 8.07 (d, J = 1.8 Hz, 1H, -ArH), 7.52 (dd, J = 8.7, 1.8 Hz, 1H, -ArH), 7.38 (d, J = 8.9 Hz, 1H, -ArH), 7.25 (d, J = 2.8 Hz, 1H, -ArH), 7.11 (dd, J = 8.9, 2.8 Hz, 1H, -ArH), 5.41 (s, 2H, -NH₂), 3.66 (t, J = 3.9 Hz, 4H, -OCH₂), 3.22 (s, 2H, -COCH₂), 2.54 (t, J = 3.6 Hz, 4H, -N-CH₂). ¹³C NMR (151 MHz, DMSO-d₆) δ 175.0, 169.1, 156.3, 147.8, 145.6, 144.0, 126.7, 122.8, 121.8, 118.4, 116.2, 115.4, 106.2, 106.1, 66.0, 62.0, 53.1. HRMS (ESI⁺) [M + H]⁺ C₁₉H₂₀N₃O₄: 354.1454, Found: 354.1430 .

N-(7-amino-9-oxo-9H-xanthen-3-yl)-2-(pyrrolidin-1-yl)acetamide (**11c**) Yellow solid, 16.5% yield. ¹H NMR (600 MHz, DMSO-d₆) δ 10.94 (s, 1H, -NH-), 8.14 (d, J = 8.7 Hz, 1H, -ArH), 8.00 (d, J = 1.6 Hz, 1H, -ArH), 7.45 (dd, J = 8.7, 1.6 Hz, 1H, -ArH), 7.40 (d, J = 8.9 Hz, 1H, -ArH), 7.26 (d, J = 2.8 Hz, 1H, -ArH), 7.13 (dd, J = 8.9, 2.8 Hz, 1H, -ArH), 5.44 (s, 2H, -NH₂), 3.11 (s, 2H, -COCH₂), 2.05–1.80 (m, 8H, -CH₂). ¹³C NMR (151 MHz, DMSO-d₆) δ 175.0, 165.3, 156.2, 147.7, 145.7, 143.4, 127.1, 122.9, 121.8, 118.5, 116.6, 115.2, 106.3, 106.2, 63.3, 54.3, 22.8. HRMS (ESI⁺) [M + H]⁺ C₁₉H₂₀N₃O₃: 338.1505, Found: 338.1477 .

N-(7-amino-9-oxo-9H-xanthen-3-yl)-2-(4-methylpiperazin-1-yl)acetamide (**11d**) Yellow solid, 10.45% yield. ¹H NMR (600 MHz, DMSO-d₆) δ 10.23 (s, 1H, -NH-), 8.08 (d, J = 9.9 Hz, 2H, Ar-H), 7.51 (dd, J = 8.7, 1.3 Hz, 1H, Ar-H), 7.38 (d, J = 8.9 Hz, 1H, Ar-H), 7.26 (d, J = 2.7 Hz, 1H, Ar-H), 7.11 (dd, J = 8.9, 2.7 Hz, 1H, Ar-H), 5.41 (s, 2H, -NH₂), 3.20 (s, 2H, -COCH₂), 2.51 (s, 4H, -CH₂), 2.43–2.35 (m, 4H, -CH₂), 2.18 (s, 3H, -CH₃). ¹³C NMR (151 MHz, DMSO-d₆) δ 175.0, 169.4, 156.3, 147.8, 145.6, 144.1, 126.7, 122.8, 121.8, 118.4, 116.2, 115.4, 106.2, 106.0, 61.8, 54.4, 52.6, 45.7. HRMS (ESI⁺) [M + H]⁺ C₂₀H₂₃N₄O₃: 367.1770, Found: 367.1750.

N-(7-amino-9-oxo-9H-xanthen-3-yl)-2-(4-ethylpiperazin-1-yl)acetamide (**11e**) Yellow solid, 13.4% yield. ¹H NMR (600 MHz, DMSO-d₆) δ 13.28 (s, 1H, -NH), 8.59 (d, J = 8.2 Hz, 1H, Ar-H), 7.72 (t, J = 8.4 Hz, 1H, Ar-H), 7.38 (d, J = 8.9 Hz, 1H, Ar-H), 7.28 (d, J = 2.6 Hz, 1H, Ar-H), 7.23 (d, J = 8.8 Hz, 1H, Ar-H), 7.17 (dd, J = 8.8, 2.6 Hz, 1H, Ar-H), 5.50 (s, 2H, -NH₂), 3.22 (s, 2H, -COCH₂), 2.65 (d, J = 35.9 Hz, 8H, -CH₂-), 2.39 (d, J = 4.1 Hz, 2H, -CH₂-), 1.08 (t, J = 7.1 Hz, 3H, -CH₃), ¹³C NMR (151 MHz, DMSO-d₆) δ 178.9, 170.2, 156.3, 146.8, 145.8, 140.3, 135.3, 123.7, 121.7, 118.1, 112.5, 111.6, 108.8, 105.7, 62.2, 52.7, 51.9, 51.6, 11.8, HRMS (ESI⁺) [M + H]⁺ C₂₁H₂₅N₄O₃: 381.1927, Found: 381.1889.

N-(7-amino-9-oxo-9H-xanthen-3-yl)-2-(2-methylpiperidin-1-yl)acetamide (**11f**) Yellow solid, 18.6% yield. ¹H NMR (600 MHz, DMSO-d₆) δ 10.16 (s, 1H, -NH), 8.10 (s, 1H, Ar-H), 8.08 (s, 1H, Ar-H), 7.57–7.51 (m, 1H, Ar-H), 7.38 (d, J = 8.9 Hz, 1H, Ar-H), 7.26 (d, J = 2.8 Hz, 1H, Ar-H), 7.12 (dd, J = 8.9, 2.8 Hz, 1H, Ar-H), 5.41 (s, 2H, -NH₂), 3.17 (s, 2H, -COCH₂), 2.84 (s, 1H, -N-CH), 1.64 (s, 2H, -CH₂), 1.57 (s, 2H, -CH₂), 1.35–1.23 (m, 2H, -CH₂), 1.24 (d, J = 9.9 Hz, 2H, -CH₂), 1.05 (s, 3H, -CH₃). ¹³C NMR (151 MHz, DMSO-d₆) δ 175.0, 163.7,

156.3, 147.8, 145.6, 143.9, 126.8, 122.8, 121.8, 118.4, 116.2, 115.4, 106.2, 106.0, 53.3, 49.2, 48.6, 31.1, 30.3, 29.8, 18.8. HRMS (ESI⁺) [M + H]⁺ C₂₁H₂₄N₃O₃: 366.1818, Found: 366.1789.

N-(7-amino-9-oxo-9H-xanthen-3-yl)-2-(piperidin-1-yl)acetamide (**11g**) Yellow solid, 9.5% yield. ¹H NMR (600 MHz, DMSO-d₆) δ 10.37 (s, 1H, -NH), 8.10 (d, J = 8.7 Hz, 1H, Ar-H), 8.06 (s, 1H, Ar-H), 7.51 (d, J = 8.7 Hz, 1H, Ar-H), 7.39 (d, J = 8.9 Hz, 1H, Ar-H), 7.26 (d, J = 2.6 Hz, 1H, Ar-H), 7.12 (dd, J = 8.8, 2.6 Hz, 1H, Ar-H), 5.42 (s, 2H, -NH₂), 2.68 (s, 2H, -COCH₂), 2.51 (s, 4H, -N-CH₂), 1.67–1.60 (m, 4H, -CH₂), 1.44 (s, 2H, -CH₂). ¹³C NMR (151 MHz, DMSO-d₆) δ 175.0, 172.0, 156.3, 147.8, 145.6, 143.8, 126.8, 122.8, 121.8, 118.4, 116.3, 115.4, 106.2, 106.1, 61.1, 53.8, 22.1, 21.0. HRMS (ESI⁺) [M + H]⁺ C₂₀H₂₂N₃O₃: 352.1661, Found: 352.1627.

N-(7-amino-9-oxo-9H-xanthen-3-yl)-3-(diethylamino)propanamide (**12a**) Yellow solid, 25.4% yield. ¹H NMR (600 MHz, DMSO-d₆) δ 10.69 (s, 1H, -NH), 8.08 (d, J = 8.7 Hz, 1H, Ar-H), 8.04 (d, J = 1.3 Hz, 1H, Ar-H), 7.38 (d, J = 8.9 Hz, 1H, Ar-H), 7.11 (dd, J = 8.7, 1.3 Hz, 1H, Ar-H), 7.25 (d, J = 2.8 Hz, 1H, Ar-H), 7.11 (dd, J = 8.9, 2.8 Hz, 1H, Ar-H), 5.41 (s, 2H, -NH₂), 3.17 (s, 2H, -COCH₂), 2.80 (s, 2H, -CH₂), 2.53 (q, J = 6.6 Hz, 4H, -CH₂), 0.99 (t, J = 7.1 Hz, 6H, CH₃). ¹³C NMR (151 MHz, DMSO-d₆) δ 175.0, 171.4, 156.4, 147.8, 145.6, 144.6, 126.8, 122.7, 121.8, 118.4, 116.0, 115.0, 106.3, 105.6, 48.1, 46.1, 34.2, 11.6. HRMS (ESI⁺) [M + H]⁺ C₂₀H₂₄N₃O₃: 354.1818, Found: 354.1799.

N-(7-amino-9-oxo-9H-xanthen-3-yl)-3-morpholinopropanamide (**12b**) Yellow solid, 35.1% yield. ¹H NMR (600 MHz, DMSO-d₆) δ 10.58 (s, 1H, -NH), 8.08 (d, J = 8.7 Hz, 1H, Ar-H), 8.04 (d, J = 1.6 Hz, 1H, Ar-H), 7.38 (d, J = 8.8 Hz, 2H, Ar-H), 7.25 (d, J = 2.8 Hz, 1H, Ar-H), 7.11 (dd, J = 8.9, 2.8 Hz, 1H, Ar-H), 5.41 (s, 2H, -NH₂), 3.58 (t, J = 4.2 Hz, 4H, -OCH₂), 2.66 (t, J = 7.0 Hz, 2H, -CH₂), 2.57 (t, J = 7.0 Hz, 2H, -COCH₂), 2.42 (t, J = 4.2 Hz, 4H, -N-CH₂). ¹³C NMR (151 MHz, DMSO-d₆) δ 175.0, 171.1, 156.4, 147.8, 145.6, 144.6, 126.8, 122.7, 121.8, 118.4, 116.0, 115.1, 106.3, 105.7, 66.2, 53.9, 53.0, 34.1. HRMS (ESI⁺) [M + H]⁺ C₂₀H₂₂N₃O₄: 368.1610, Found: 368.1593.

N-(7-amino-9-oxo-9H-xanthen-3-yl)-3-(pyrrolidin-1-yl)propanamide (**12c**), Yellow solid, 12.4% yield. ¹H NMR (600 MHz, DMSO-d₆) δ 10.85 (s, 1H, -NH), 8.07 (d, J = 8.7 Hz, 2H, Ar-H), 7.42 (dd, J = 8.7, 1.8 Hz, 1H, Ar-H), 7.38 (d, J = 8.9 Hz, 1H, Ar-H), 7.25 (d, J = 2.8 Hz, 1H, Ar-H), 7.10 (dd, J = 8.9, 2.8 Hz, 1H, Ar-H), 5.41 (s, 2H, -NH₂), 2.74 (t, J = 7.0 Hz, 2H, -CH₂), 2.57 (t, J = 7.0 Hz, 2H, -COCH₂), 2.49–2.47 (m, 4H, -CH₂), 1.69–1.67 (m, 4H, -CH₂). ¹³C NMR (151 MHz, DMSO-d₆) δ 175.0, 171.4, 156.4, 147.8, 145.6, 144.9, 126.7, 122.7, 121.8, 118.4, 115.9, 115.2, 106.2, 105.6, 53.4, 51.3, 36.2, 23.1. HRMS (ESI⁺) [M + H]⁺ C₂₀H₂₂N₃O₃: 352.1661, Found: 352.1640.

N-(7-amino-9-oxo-9H-xanthen-3-yl)-3-(4-methylpiperazin-1-yl)propanamide (**12d**) Yellow solid, 8.4% yield. ¹H NMR (600 MHz, DMSO-d₆) δ 10.57 (s, 1H, -NH), 8.08 (d, J = 8.7 Hz, 1H, Ar-H), 8.04 (d, J = 1.5 Hz, 1H, Ar-H), 7.38 (d, J = 8.9 Hz, 2H, Ar-H), 7.25 (d, J = 2.8 Hz, 1H, Ar-H), 7.11 (dd, J = 8.9, 2.8 Hz, 1H, Ar-H), 5.41 (s, 2H, -NH₂), 3.34 (s, 2H, -CH₂), 2.71 (t, J = 7.2 Hz, 4H, -CH₂), 2.58 (t, J = 6.8 Hz, 4H, -CH₂), 2.50 (s, 2H, -

COCH₂), 2.39 (s, 3H, -CH₃). ¹³C NMR (151 MHz, DMSO-d₆) δ 175.0, 170.8, 156.4, 147.8, 145.6, 144.5, 126.8, 122.8, 121.8, 118.4, 116.0, 115.1, 106.2, 105.7, 52.9, 52.6, 49.9, 42.9, 34.1. HRMS (ESI⁺) [M + H]⁺ C₂₁H₂₅N₄O₃: 381.1927, Found: 381.1903.

N-(7-amino-9-oxo-9H-xanthen-3-yl)-3-(4-ethylpiperazin-1-yl)propanamide (**12e**) Yellow solid, 7.9% yield. ¹H NMR (600 MHz, DMSO-d₆) δ 10.55 (s, 1H, -NH), 8.08 (d, J = 8.7 Hz, 1H, Ar-H), 8.04 (d, J = 1.4 Hz, 1H, Ar-H), 7.40 (dd, J = 8.7, 1.5 Hz, 1H, Ar-H), 7.38 (d, J = 8.9 Hz, 1H, Ar-H), 7.25 (d, J = 2.7 Hz, 1H, Ar-H), 7.11 (dd, J = 8.9, 2.8 Hz, 1H, Ar-H), 5.40 (s, 2H, -NH₂), 3.32 (s, 2H, -CH₂), 3.17 (s, 2H, -COCH₂), 3.09–2.71 (m, 8H, -CH₂), 2.61 (s, 2H, -CH₂), 1.15 (s, 3H, -CH₃). ¹³C NMR (151 MHz, DMSO-d₆) δ 174.8, 170.9, 156.2, 147.6, 145.4, 144.4, 126.6, 122.6, 121.6, 118.2, 115.8, 114.9, 106.1, 105.5, 53.0, 51.6, 51.4, 51.4, 51.1, 43.0, 33.9, 10.9. HRMS (ESI⁺) [M + H]⁺ C₂₂H₂₇N₄O₃: 395.2083, Found: 395.2061.

N-(7-amino-9-oxo-9H-xanthen-3-yl)-3-(2-methylpiperidin-1-yl)propanamide (**12f**), Yellow solid, 23.4% yield. ¹H NMR (600 MHz, DMSO-d₆) δ 10.70 (s, 1H, -NH), 8.11 (d, J = 8.7 Hz, 1H, Ar-H), 8.04 (d, J = 1.3 Hz, 1H, Ar-H), 7.43 (d, J = 8.7 Hz, 1H, Ar-H), 7.39 (d, J = 8.9 Hz, 1H, Ar-H), 7.25 (d, J = 2.8 Hz, 1H, Ar-H), 7.12 (dd, J = 8.9, 2.8 Hz, 1H, Ar-H), 5.42 (s, 2H, -NH₂), 3.17–3.16 (m, 1H, -CH-), 2.91 (s, 2H, -CH₂), 2.52–2.51 (m, 2H, -CH₂), 2.51–2.50 (m, 2H, -COCH₂), 1.90–1.43 (m, 6H, -CH₂), 1.40–1.25 (m, 3H, -CH₃). ¹³C NMR (151 MHz, DMSO-d₆) δ 175.0, 171.1, 156.3, 147.8, 145.6, 144.3, 126.9, 122.8, 121.8, 118.4, 116.2, 115.1, 106.2, 105.9, 64.8, 58.8, 48.8, 36.2, 31.4, 26.8, 21.1, 15.3. HRMS (ESI⁺) [M + H]⁺ C₂₂H₂₆N₃O₃: 380.1969, Found: 380.1953.

4.2 Antiproliferative activity using MTT assay

MTT method was used to detect the growth inhibitory effects of the compounds on MCF-7, Hela, MGC-803 cell lines and normal cells L929. Inoculate the cells in a 96-well cell culture plate containing complete medium at a cell density of 5×10⁴ cells per well, and incubated for 12 h, then treated with the compounds (predissolved in DMSO) at a five-dose assay ranging from 5 to 120 μM (2.5–30 μM for etoposide and 0.05–1.5 μM for adriacin and camptothecine). After 48 h incubation at 37°C, MTT solution (10 μL, 5 mg/mL) in PBS (PBS without MTT as the blank) was fed to each well of the culture plate (containing 100 μL medium). After 4 h incubation, remove the medium and MTT, then add 100 μL DMSO to dissolve the crystals. Measure the absorbance of each well at OD_{490nm} with a Bio-Tek microplate Reader. All experiments were performed in triplicate and each experiment was repeated at least three times. The IC₅₀ values were calculated by nonlinear regression analysis (GraphPad Prism).

4.3 DNA topoisomerase I inhibition assay *in vitro*

The supercoiled DNA pBR322 (TaKaRa Bio) relaxation experiment was used to detect the effect of the compound on the activity of DNA topoisomerase I. The experimental method refers to previous reports^[44]. Add 1U of DNA topoisomerase I (TaKaRa Bio), 250 ng of supercoiled DNA pBR322, 2 μL of a reaction 10×buffer (TaKaRa Bio) (35 mM Tris-HCl, pH 8, 72 mM KCl, 5 mM MgCl₂, 5 mM DTT) to the reaction

system, 5 mM spermidine, 0.01% BSA) and different concentrations of the test compound dissolved in DMSO in advance and the control camptothecin. The mixture was incubated at 37°C for 30 min, and then the reaction was terminated by adding 2 μ L of 10% SDS solution, 1 μ L of DNA loading buffer. The reaction product was subjected to 1% agarose gel electrophoresis in the absence or presence of ethidium bromide (0.5 μ g/mL). When the agarose gel electrophoresis was performed in the absence of ethidium bromide, the gel was stained with 0.5 μ g/mL ethidium bromide after electrophoresis.

4.4 DNA topoisomerase II inhibition assay *in vitro*

Topoisomerase II was purified and extracted from the nuclei from MGC-803 cells as described previously^[45]. The reaction mixture of pBR322 (250 ng) and Topoisomerase II (1 unit) was incubated with etoposide, compounds (100 μ M or 20 μ M) in a final volume of 10 μ L in Topo II reaction buffer (Tris-HCl (50 mM, pH 8.0), NaCl (150 mM), MgCl₂ (10 mM), dithiothreitol (0.5 mM), ATP (2 mM)) for 30 min at 37°C. And then the reaction was terminated by adding 1 μ L of 10% SDS solution, 1 μ L of 6 \times DNA loading buffer. Electrophoresis was performed on a 1% agarose gel at 83 V for 55 min in TBE buffer (Tris-borate and EDTA). Gels were stained for 15 min in an aqueous solution of EB (0.5 μ g/mL) and photographed under UV light (Tanon-1600 Gel Imaging System).

4.5 UV-Visible titration assay

The ctDNA solution was prepared in 10mM Tris-HCl buffer solution (pH = 7.4). In order to verify whether the DNA is purified, the UV absorbance of the DNA was measured at 260 nm and 280 nm. The results showed that the absorbance of the DNA at these two wavelengths was greater than 1.8, indicating that the DNA does not contain protein and meets the experimental requirements. The concentration of ctDNA was determined by UV absorbance at 260nm using a molar absorptivity constant of 6600 L \cdot mol⁻¹ \cdot cm⁻¹. Compounds **7d** (**7e**, **8d** and **8e**) were dissolved in 3 mL Tris-HCl buffer solution in the present or absence of increasing concentration of ctDNA (0, 50, 100, 150, 200, 250 μ M). Absorption spectra were recorded in the wavelength range of 200–400 nm after equilibration at room temperature for 5 min using UV visible spectro photometer (T6 new century ultraviolet - visible spectrophotometer, Beijing Purkay General Instrument Co. Ltd).

4.6 EB displacement assay

In brief, increasing concentration (0, 50, 100, 150, 200, 250, 300, 350, 400 μ M) of **7d** (**7e**, **8d**, and **8e**) was added to samples containing 200 ng pBR322 DNA plasmid and 2.5mM EB in a fluorescence buffer (10 mM Tris-HCl, pH = 7.4). Fluorescence emission spectra were obtained for each **7d** (**7e**, **8d**, and **8e**) concentration.

4.7 DNA unwinding assay

DNA relaxation experiment mediated by topoisomerase I: treating negatively supercoiled pBR322 with Topo I in Topo I reaction (35 mM pH 8 Tris-HCl, 72 mM KCl, 5 mM MgCl₂, 5 mM DTT, 5 mM spermidine,

0.01% BSA) buffer at 37°C for 30 min. Then add 1 µL 10% SDS to the reaction system to stop the reaction, and incubate at 37°C for 60 min. Finally, add EB and diluted test compound **7d** (**7e**) or **8d** (**8e**) to the reaction system, and incubate at 37°C for 30 min. After addition of loading buffer, electrophoresis was performed on a 1% agarose gel at 83 V for 60 min in TBE buffer (Tris-borate and EDTA). Gels were stained for 15 min in an aqueous solution of EB (0.5 µg/mL) and photographed under UV light (Tanon-1600 Gel Imaging System).

4.8 Cell apoptotic analysis

Flow cytometric analysis was performed to evaluate the cell apoptotic analysis. MGC-803 (5×10^4) cells were seeded in six-well plates and allowed to grow 24 h. The medium was then replaced with complete medium containing compounds **7d** and **8d** at 2.5 and 10 µM concentrations for 48 h. After 48 h of compound treatment, cells from the supernatant and adherent monolayer cells were harvested by trypsinization, washed with PBS at 1200 rpm. Then the cells were stained with Annexin-VFITC/PI (Solarbio). Then the samples were analyzed by flow cytometry (BD FACS Caliber instrument) as described earlier^[42].

4.9 Cell cycle analysis

Flow cytometry was performed to analyze the distribution of cell cycles. MGC-803 cells were treated with compounds **7d** and **8d** at 2.5 and 5 µM concentrations for 48 h. Untreated and treated cells were harvested, washed with phosphate-buffered saline (PBS), fixed in ice-cold 75% ethanol, and stained with RNaseA/PI (Solarbio). Cell-cycle analysis was performed by flow cytometry.

4.10 Molecular Docking

In order to further explore the mode of action between the compound and topoisomerase II, molecular docking was used to study, and the maestro software was used for the docking. Draw the **7d** and **8d** molecular structures and transformed them into three-dimensional structures and minimized energy. The X-ray structures of the human topoisomerase II (PDB ID: 4G0V) and DNA (PDB ID: 2DES) were obtained from the RCSB protein database (<http://www.rcsb.org>). The ligands were prepared by Ligprep module. The proteins were prepared, optimized and minimized using pre-process method of Prepviz module of Maestro molecular modeling with default parameters. All the water molecules and ligands were removed and the hydrogen atoms were added. The grid box was generated around the centroid of the co-crystallized ligand at the Mitoxantrone/Adriamycin binding site. The prepared ligands and protein/DNA were docked using the Glide module with the standard precision.

Declarations

Acknowledgments

We gratefully acknowledge Natural Science Foundation of Science and Technology Project of Hebei Education Department (ZD2019060); Hebei Province (B2018201269 and B2019201359); National Natural Science Foundation of China (82003597); Institute of Life Science and Green Development; Natural Science Interdisciplinary Research Program of Hebei University (DXK201912); Post-graduate's Innovation Found Project of Hebei Province (CXZZSS2021012) and Project of Hebei University Student Innovation and Entrepreneurship Training Program (2021193) for financial support; And this work also supported by the High-Performance Computing Center of Hebei University.

Conflict of Interest

The authors declare that they have no known competing financial interests or personal relationships that could have appeared to influence the work reported in this paper.

References

1. Jaracz S, Chen J, Kuznetsova LV, Ojima I. Recent advances in tumor-targeting anticancer drug conjugates. *Bioorganic & medicinal chemistry*. 2005;13(17):5043-54. doi:10.1016/j.bmc.2005.04.084.
2. Li PH, Zeng P, Chen SB, Yao PF, Mai YW, Tan JH *et al*. Synthesis and Mechanism Studies of 1,3-Benzoazolyl Substituted Pyrrolo[2,3-b]pyrazine Derivatives as Nonintercalative Topoisomerase II Catalytic Inhibitors. *J Med Chem*. 2016;59(1):238-52. doi:10.1021/acs.jmedchem.5b01284.
3. Sangpheak K, Mueller M, Darai N, Wolschann P, Suwattanasophon C, Ruga R *et al*. Computational screening of chalcones acting against topoisomerase II α and their cytotoxicity towards cancer cell lines. *Journal of enzyme inhibition and medicinal chemistry*. 2019;34(1):134-43. doi:10.1080/14756366.2018.1507029.
4. Sheng J, Gan J, Huang Z. Structure-based DNA-targeting strategies with small molecule ligands for drug discovery. *Medicinal research reviews*. 2013;33(5):1119-73. doi:10.1002/med.21278.
5. Deady LW, Kaye AJ, Finlay GJ, Baguley BC, Denny WA. Synthesis and antitumor properties of N-[2-(dimethylamino)ethyl]carboxamide derivatives of fused tetracyclic quinolines and quinoxalines: a new class of putative topoisomerase inhibitors. *J Med Chem*. 1997;40(13):2040-6. doi:10.1021/jm970044r.
6. Hu W, Huang XS, Wu JF, Yang L, Zheng YT, Shen YM. Discovery of Novel Topoisomerase II Inhibitors by Medicinal Chemistry Approaches. *J Med Chem*. 2018;61(20):8947-80. doi:10.1021/acs.jmedchem.7b01202.
7. Dileep KV, Vijeesh V, Remya C. Rational design and interaction studies of combilexins towards duplex DNA. *Molecular bioSystems*. 2016;12(3):860-7. doi:10.1039/c5mb00808e.
8. Zhou DC, Lu YT, Mai YW, Zhang C, Xia J, Yao PF *et al*. Design, synthesis and biological evaluation of novel perimidine o-quinone derivatives as non-intercalative topoisomerase II catalytic inhibitors.

Bioorganic chemistry. 2019;91:103131. doi:10.1016/j.bioorg.2019.103131.

9. Jun KY, Kwon H, Park SE, Lee E, Karki R, Thapa P *et al.* Discovery of dihydroxylated 2,4-diphenyl-6-thiophen-2-yl-pyridine as a non-intercalative DNA-binding topoisomerase II-specific catalytic inhibitor. *European journal of medicinal chemistry*. 2014;80:428-38. doi:10.1016/j.ejmech.2014.04.066.
10. Chen W, Shen Y, Li Z, Zhang M, Lu C, Shen Y. Design and synthesis of 2-phenylnaphthalenoids as inhibitors of DNA topoisomerasella and antitumor agents. *European journal of medicinal chemistry*. 2014;86:782-96. doi:10.1016/j.ejmech.2014.08.073.
11. Wang JC, Kirkegaard K. DNA topoisomerases. *Gene amplification and analysis*. 1981;2:455-73.
12. Pommier Y. DNA topoisomerase I inhibitors: chemistry, biology, and interfacial inhibition. *Chemical reviews*. 2009;109(7):2894-902. doi:10.1021/cr900097c.
13. Champoux JJ. DNA topoisomerases: structure, function, and mechanism. *Annual review of biochemistry*. 2001;70:369-413. doi:10.1146/annurev.biochem.70.1.369.
14. Wei H, Ruthenburg AJ, Bechis SK, Verdine GL. Nucleotide-dependent domain movement in the ATPase domain of a human type IIA DNA topoisomerase. *The Journal of biological chemistry*. 2005;280(44):37041-7. doi:10.1074/jbc.M506520200.
15. Hu W, Huang XS, Wu JF, Yang L, Zheng YT, Shen YM. Discovery of Novel Topoisomerase II Inhibitors by Medicinal Chemistry Approaches. 2018;61(20):8947-80. doi:10.1021/acs.jmedchem.7b01202.
16. Creemers GJ, Lund B, Verweij J. Topoisomerase I inhibitors: topotecan and irinotecan. *Cancer treatment reviews*. 1994;20(1):73-96. doi:10.1016/0305-7372(94)90011-6.
17. Pogorelčnik B, Janežič M, Sosič I, Gobec S, Solmajer T, Perdih A. 4,6-Substituted-1,3,5-triazin-2(1H)-ones as monocyclic catalytic inhibitors of human DNA topoisomerase II α targeting the ATP binding site. *Bioorganic & medicinal chemistry*. 2015;23(15):4218-29. doi:10.1016/j.bmc.2015.06.049.
18. Chang SM, Christian W, Wu MH, Chen TL, Lin YW, Suen CS *et al.* Novel indolizino[8,7-b]indole hybrids as anti-small cell lung cancer agents: Regioselective modulation of topoisomerase II inhibitory and DNA crosslinking activities. *European journal of medicinal chemistry*. 2017;127:235-49. doi:10.1016/j.ejmech.2016.12.046.
19. Jadala C, Sathish M, Reddy TS, Reddy VG, Tokala R, Bhargava SK *et al.* Synthesis and in vitro cytotoxicity evaluation of β -carboline-combretastatin carboxamides as apoptosis inducing agents: DNA intercalation and topoisomerase-II inhibition. *Bioorganic & medicinal chemistry*. 2019;27(15):3285-98. doi:10.1016/j.bmc.2019.06.007.
20. Liu C, Zhang M, Zhang Z, Zhang SB, Yang S, Zhang A *et al.* Synthesis and anticancer potential of novel xanthone derivatives with 3,6-substituted chains. *Bioorganic & medicinal chemistry*.

2016;24(18):4263-71. doi:10.1016/j.bmc.2016.07.020.

21. Zou H, Koh JJ, Li J, Qiu S, Aung TT, Lin H *et al.* Design and synthesis of amphiphilic xanthone-based, membrane-targeting antimicrobials with improved membrane selectivity. *J Med Chem.* 2013;56(6):2359-73. doi:10.1021/jm301683j.

22. Kelly JX, Winter R, Peyton DH, Hinrichs DJ, Riscoe M. Optimization of xanthenes for antimalarial activity: the 3,6-bis-omega-diethylaminoalkoxyxanthone series. *Antimicrobial agents and chemotherapy.* 2002;46(1):144-50. doi:10.1128/aac.46.1.144-150.2002.

23. Qin J, Lan W, Liu Z, Huang J, Tang H, Wang H. Synthesis and biological evaluation of 1, 3-dihydroxyxanthone mannich base derivatives as anticholinesterase agents. *Chemistry Central journal.* 2013;7(1):78. doi:10.1186/1752-153x-7-78.

24. Waszkielewicz AM, Gunia A, Szkaradek N, Pytka K, Siwek A, Satała G *et al.* Synthesis and evaluation of pharmacological properties of some new xanthone derivatives with piperazine moiety. *Bioorganic & medicinal chemistry letters.* 2013;23(15):4419-23. doi:10.1016/j.bmcl.2013.05.062.

25. Santos CM, Freitas M, Ribeiro D, Gomes A, Silva AM, Cavaleiro JA *et al.* 2,3-diarylxanthenes as strong scavengers of reactive oxygen and nitrogen species: a structure-activity relationship study. *Bioorganic & medicinal chemistry.* 2010;18(18):6776-84. doi:10.1016/j.bmc.2010.07.044.

26. Woo S, Kang DH, Nam JM, Lee CS, Ha EM, Lee ES *et al.* Synthesis and pharmacological evaluation of new methyloxiranylmethoxyxanthone analogues. *European journal of medicinal chemistry.* 2010;45(9):4221-8. doi:10.1016/j.ejmech.2010.06.017.

27. Park SE, Chang IH, Jun KY, Lee E, Lee ES, Na Y *et al.* 3-(3-Butylamino-2-hydroxy-propoxy)-1-hydroxy-xanthen-9-one acts as a topoisomerase II α catalytic inhibitor with low DNA damage. *European journal of medicinal chemistry.* 2013;69:139-45. doi:10.1016/j.ejmech.2013.07.048.

28. Chae SW, Woo S, Park JH, Kwon Y, Na Y, Lee HJ. Xanthone analogues as potent modulators of intestinal P-glycoprotein. *European journal of medicinal chemistry.* 2015;93:237-45. doi:10.1016/j.ejmech.2015.01.006.

29. Mak NK, Li WK, Zhang M, Wong RN, Tai LS, Yung KK *et al.* Effects of euxanthone on neuronal differentiation. *Life sciences.* 2000;66(4):347-54. doi:10.1016/s0024-3205(99)00596-2.

30. Mak NK, Lung HL, Wong RN, Leung HW, Tsang HY, Leung KN. Expression of protein kinase C isoforms in euxanthone-induced differentiation of neuroblastoma cells. *Planta medica.* 2001;67(5):400-5. doi:10.1055/s-2001-15809.

31. Minniti E, Byl JAW, Riccardi L, Sissi C, Rosini M, De Vivo M *et al.* Novel xanthone-polyamine conjugates as catalytic inhibitors of human topoisomerase II α . *Bioorganic & medicinal chemistry letters.* 2017;27(20):4687-93. doi:10.1016/j.bmcl.2017.09.011.

32. Klesiewicz K, Karczewska E, Budak A, Marona H, Szkaradek N. Anti-Helicobacter pylori activity of some newly synthesized derivatives of xanthone. *The Journal of antibiotics*. 2016;69(11):825-34. doi:10.1038/ja.2016.36.
33. Han X, Zhong Y, Zhou G, Qi H, Li S, Ding Q *et al.* Synthesis and biological evaluation of N-(carbobenzyloxy)-l-phenylalanine and N-(carbobenzyloxy)-l-aspartic acid- β -benzyl ester derivatives as potent topoisomerase II α inhibitors. *Bioorganic & medicinal chemistry*. 2017;25(12):3116-26. doi:10.1016/j.bmc.2017.03.065.
34. Feng J, Qi H, Sun X, Feng S, Liu Z, Song Y *et al.* Synthesis of Novel Pyrazole Derivatives as Promising DNA-Binding Agents and Evaluation of Antitumor and Antitopoisomerases I/II Activities. *Chemical & pharmaceutical bulletin*. 2018;66(11):1065-71. doi:10.1248/cpb.c18-00546.
35. Plsikova J, Janovec L, Koval J, Ungvarsky J, Mikes J, Jendzelovsky R *et al.* 3,6-bis(3-alkylguanidino)acridines as DNA-intercalating antitumor agents. *European journal of medicinal chemistry*. 2012;57:283-95. doi:10.1016/j.ejmech.2012.09.020.
36. El-Wakil MH, El-Yazbi AF, Ashour HMA, Khalil MA, Ismail KA, Labouta IM. Discovery of a novel DNA binding agent via design and synthesis of new thiazole hybrids and fused 1,2,4-triazines as potential antitumor agents: Computational, spectrometric and in silico studies. *Bioorganic chemistry*. 2019;90:103089. doi:10.1016/j.bioorg.2019.103089.
37. Janovec L, Kožurková M, Sabolová D, Ungvarský J, Paulíková H, Plšíková J *et al.* Cytotoxic 3,6-bis((imidazolidinone)imino)acridines: synthesis, DNA binding and molecular modeling. *Bioorganic & medicinal chemistry*. 2011;19(5):1790-801. doi:10.1016/j.bmc.2011.01.012.
38. Wang BD, Yang ZY, Crewdson P, Wang DQ. Synthesis, crystal structure and DNA-binding studies of the Ln(III) complex with 6-hydroxychromone-3-carbaldehyde benzoyl hydrazone. *Journal of inorganic biochemistry*. 2007;101(10):1492-504. doi:10.1016/j.jinorgbio.2007.04.007.
39. Wang HF, Shen R, Tang N. Synthesis and characterization of the Zn(II) and Cu(II) piperidinyl isoeuxanthone complexes: DNA-binding and cytotoxic activity. *European journal of medicinal chemistry*. 2009;44(11):4509-15. doi:10.1016/j.ejmech.2009.06.019.
40. Palchaudhuri R, Hergenrother PJ. DNA as a target for anticancer compounds: methods to determine the mode of binding and the mechanism of action. *Current opinion in biotechnology*. 2007;18(6):497-503. doi:10.1016/j.copbio.2007.09.006.
41. Li D, Yuan Z, Chen S, Zhang C, Song L, Gao C *et al.* Synthesis and biological research of novel azaacridine derivatives as potent DNA-binding ligands and topoisomerase II inhibitors. *Bioorganic & medicinal chemistry*. 2017;25(13):3437-46. doi:10.1016/j.bmc.2017.04.030.

42. Song Y, Feng S, Feng J, Dong J, Yang K, Liu Z *et al.* Synthesis and biological evaluation of novel pyrazoline derivatives containing indole skeleton as anti-cancer agents targeting topoisomerase II. *European journal of medicinal chemistry*. 2020;200:112459. doi:10.1016/j.ejmech.2020.112459.
43. Shen R, Chen Y, Li Z, Qi H, Wang Y. Synthesis and biological evaluation of disubstituted amidoxanthenes as potential telomeric G-quadruplex DNA-binding and apoptosis-inducing agents. *Bioorganic & medicinal chemistry*. 2016;24(4):619-26. doi:10.1016/j.bmc.2015.12.025.
44. Lu Y, Yin W, Alam MS, Kadi AA, Jahng Y, Kwon Y *et al.* Synthesis, Biological Evaluation and Molecular Docking Study of Cyclic Diarylheptanoids as Potential Anticancer Therapeutics. *Anti-cancer agents in medicinal chemistry*. 2020;20(4):464-75. doi:10.2174/1871520619666191125130237.
45. Osheroff N, Shelton ER, Brutlag DL. DNA topoisomerase II from *Drosophila melanogaster*. Relaxation of supercoiled DNA. *The Journal of biological chemistry*. 1983;258(15):9536-43.

Schemes

Scheme 1 is available in the Supplemental Files section

Figures

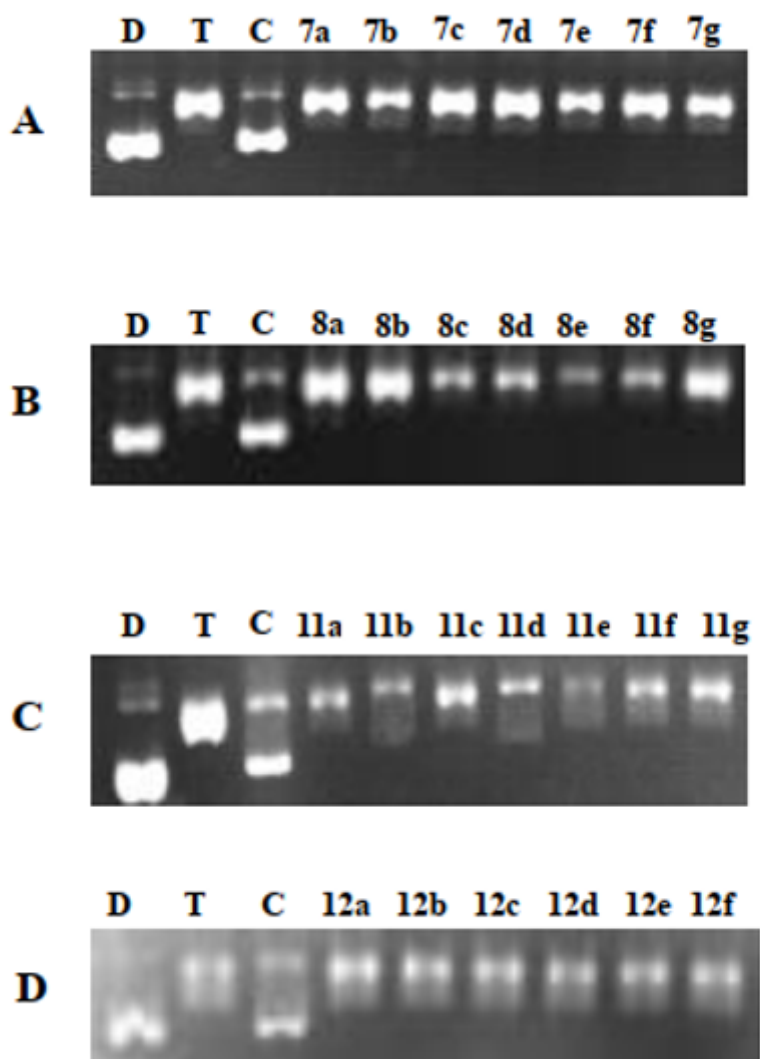


Figure 1

Human DNA topoisomerase I inhibitory activity of compounds 7a-7g, 8a-8g, 11a-11g and 12a-12f at 100 μ M. Lane D: pBR322 DNA only; lane T: pBR322 DNA + Topo I; lane C: pBR322 DNA + Topo I + Camptothecin; lanes 7a-7g, 8a-8g, 11a-11g and 12a-12f: pBR322 DNA + Topo I + compounds 7a-7g, 8a-8g, 11a-11g and 12a-12f.

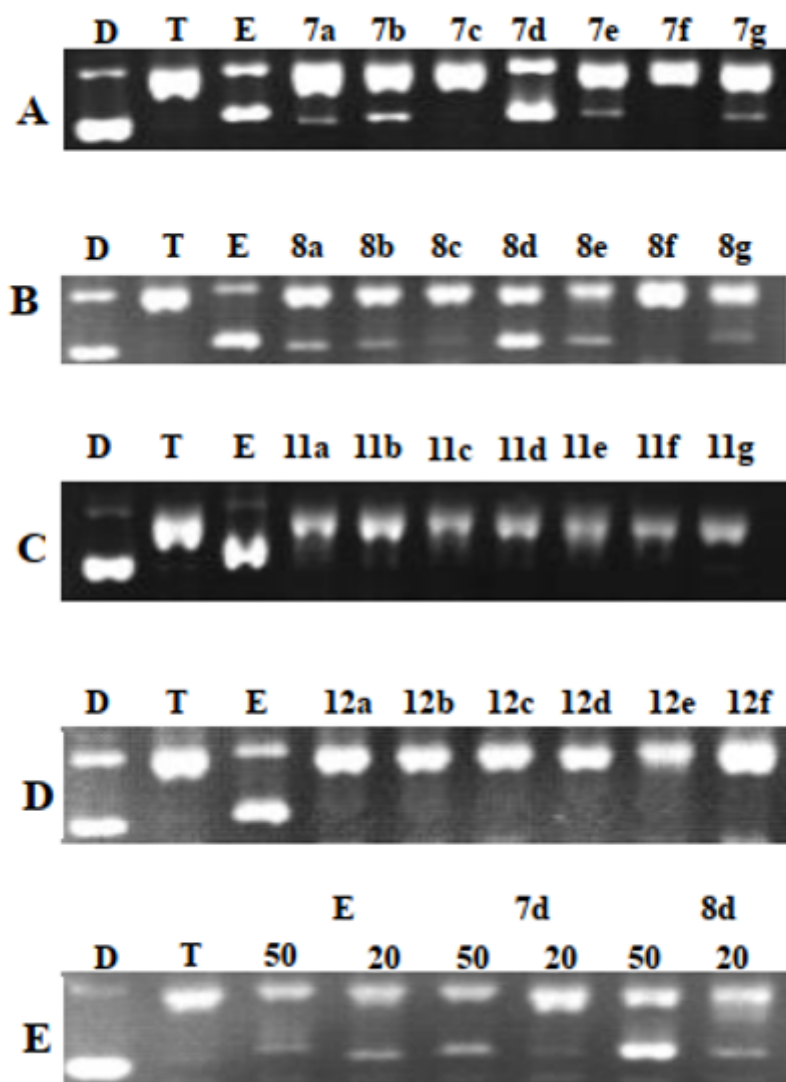


Figure 2

(A): DNA topo II inhibitory activity of compounds 7a-7g at 100 μM ; (B): DNA topo II inhibitory activity of compounds 8a-8g at 100 μM ; (C): DNA topo II inhibitory activity of compounds 11a-11g at 100 μM ; (D): DNA topo II inhibitory activity of compounds 12a-12f at 100 μM ; (E): Topo II inhibitory activity of compounds 7d and 8d at different concentrations (20, 50 μM)

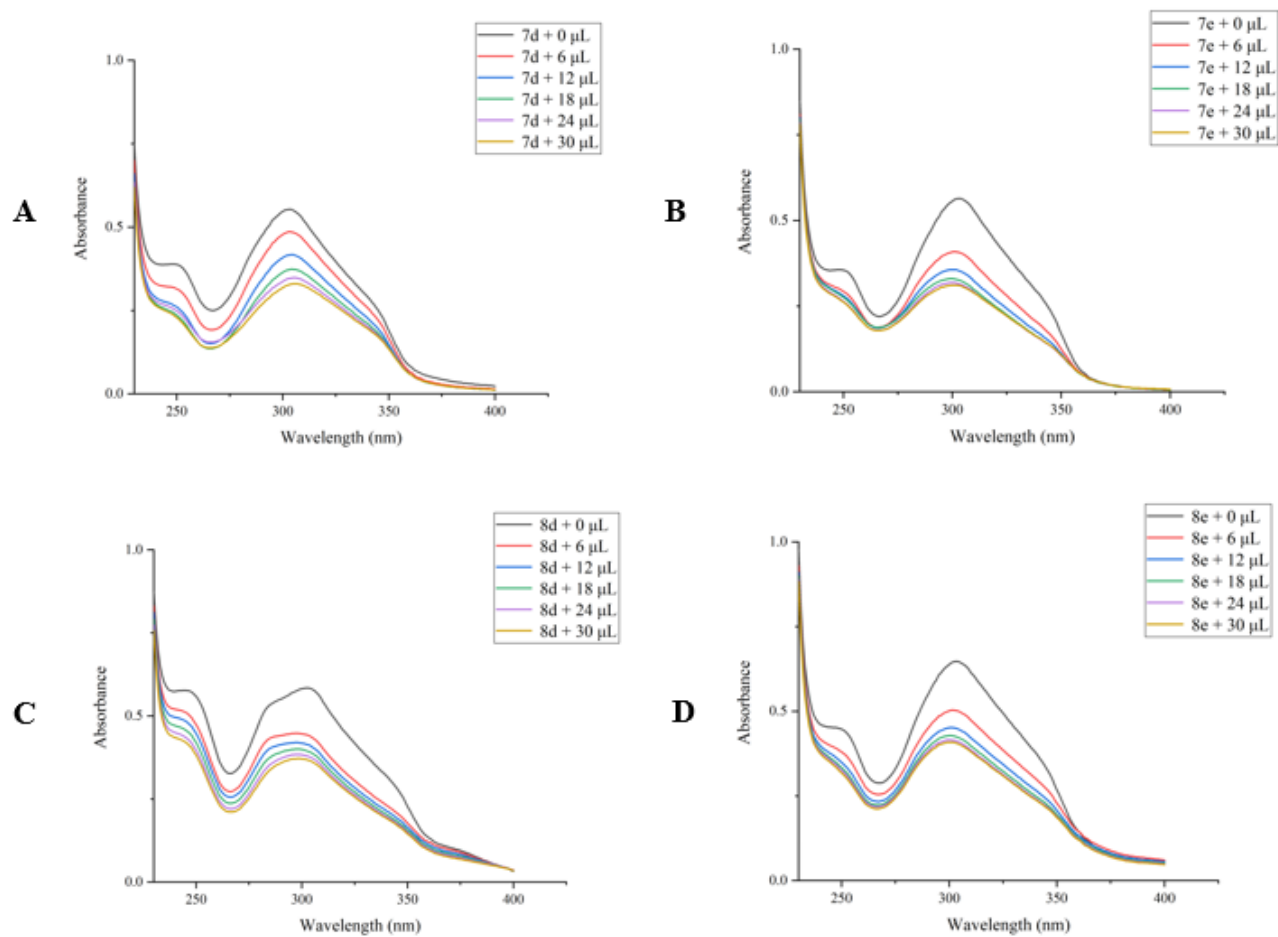


Figure 3

UV-Visible titration of tested compounds (10 mM) by increasing amounts of ctDNA; (from top to bottom 0-250 μM, at 50 μM intervals; The amount of ctDNA added to the compound is 0 μL, 6 μL, 12 μL, 18 μL, 24 μL, 30 μL). (A): 7d; (B): 7e; (C): 8d; (D): 8e.

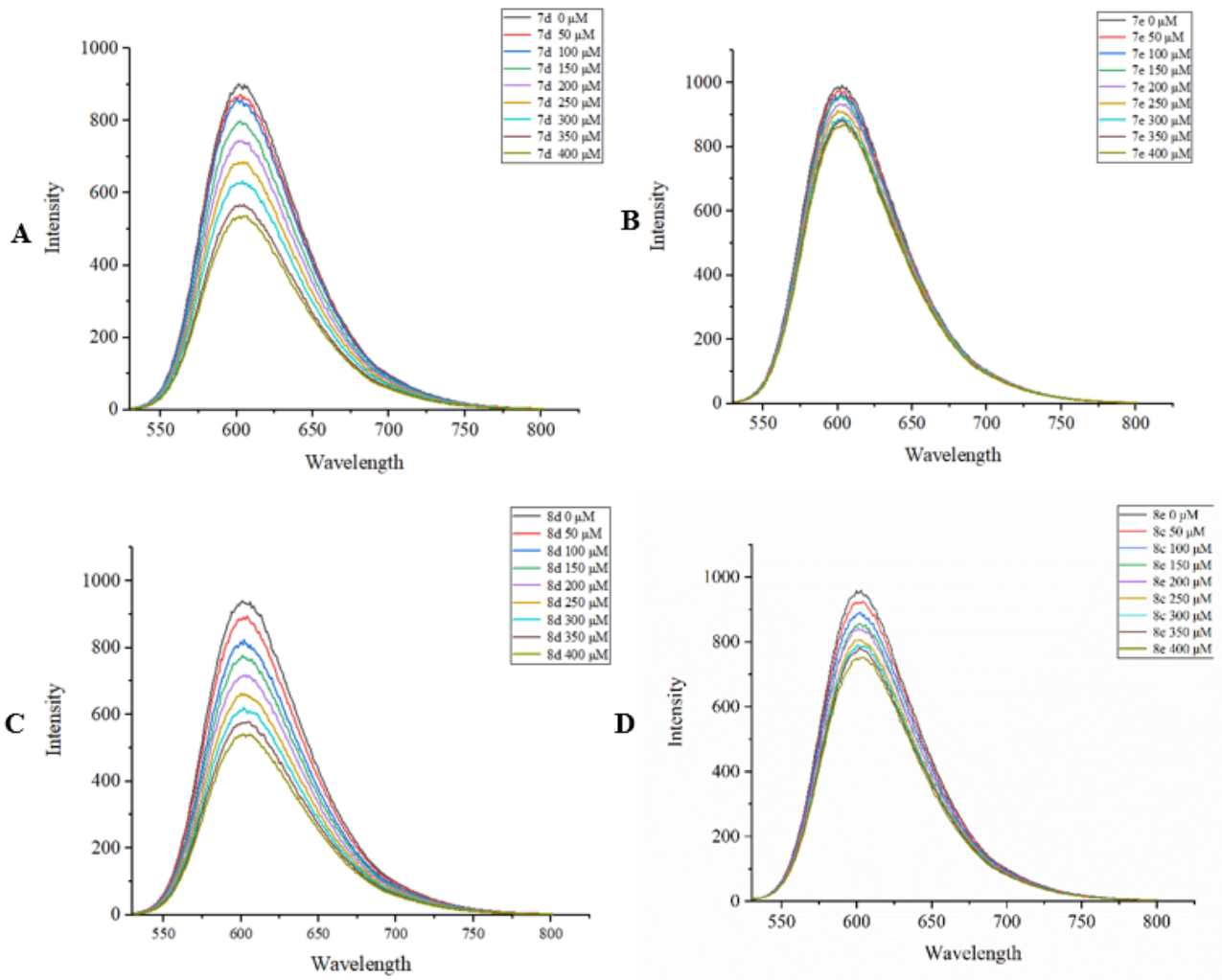


Figure 4

Fluorescence emission spectra of DNA-EB in the presence of compounds 7d, 7e, 8d, and 8e; (A): 7d; (B): 7e; (C): 8d; (D): 8e. Concentration of each substance: DNA-EB system: 2.6 μM; Compound concentration: (0, 50, 100, 150, 200, 250, 300, 350, 400 μM).

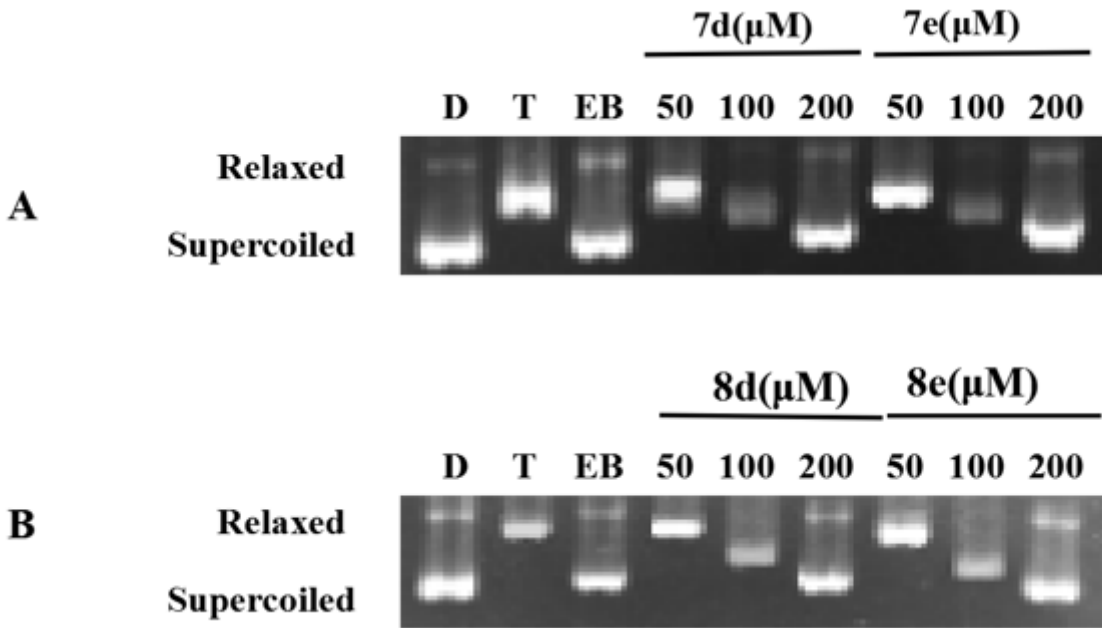


Figure 5

DNA unwinding assay. Lane D: pBR322 DNA only; lane T: pBR322 DNA + Topo I; lane EB: pBR322 DNA + Topo I + EB; lanes 50-200: pBR322 DNA + Topo I + different concentrations compounds 7d, 7e, 8d and 8e

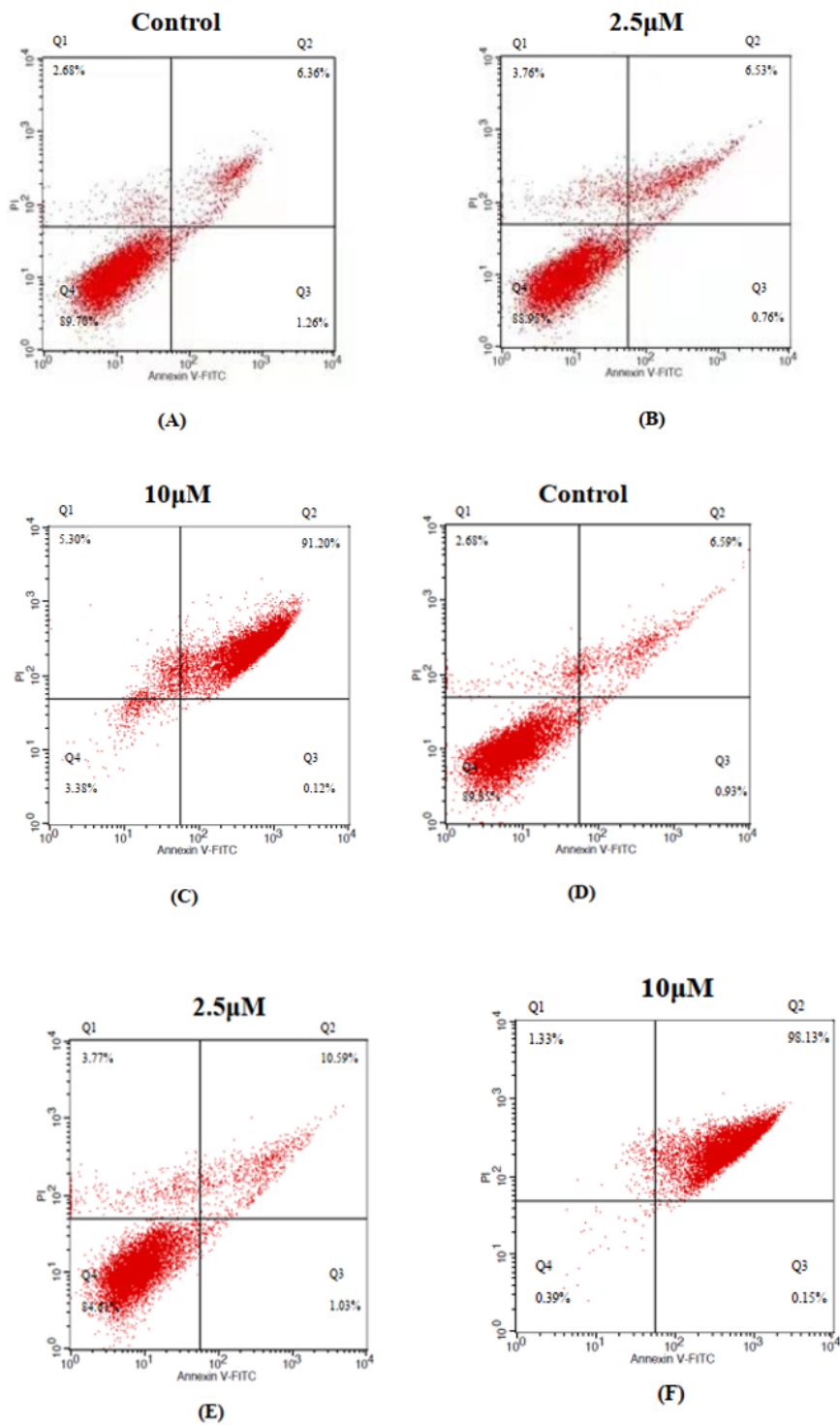
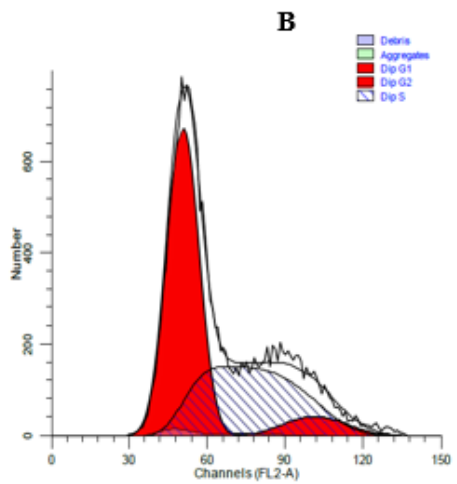
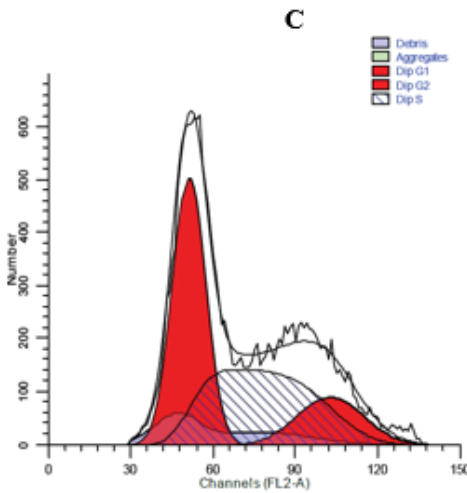
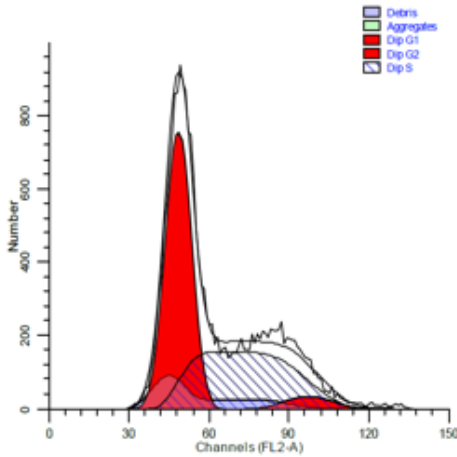
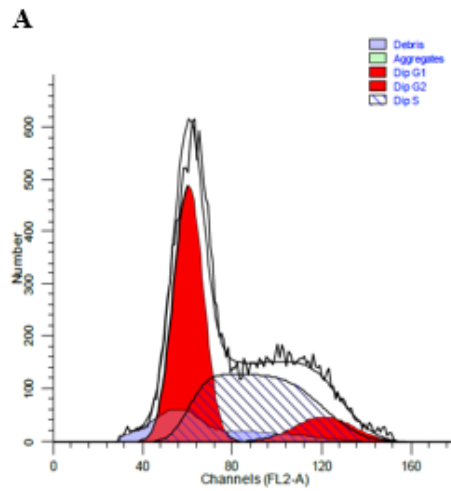
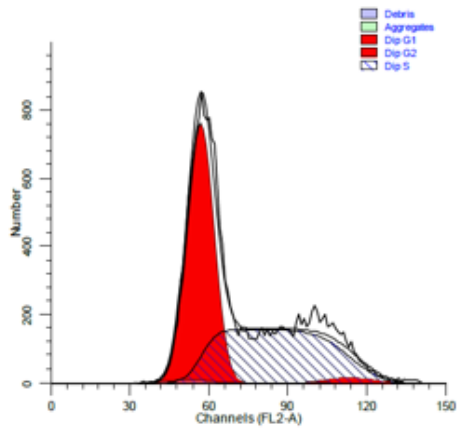


Figure 6

Annexin V-FITC/PI (AV/PI) dual staining assay: Quadrants; Upper left (necrotic cells), Lower left (live cells), Lower right (early apoptotic cells) and Upper right (late apoptotic cells). (A): control cells (MGC-803); (B): 7d(2.5 μ M); (C): 7d(10 μ M); (D): control cells (MGC-803); (E): 8d(2.5 μ M); (F): 8d(10 μ M).



D

E

Figure 7

Cell cycle analysis in MGC-803 cells after treatment with compounds 7d and 8d concentrations for 48 h. (A): Control cells, (B): 7d \times 2.5 μ M; (C): 7d \times 5 μ M; (D): 8d \times 2.5 μ M; (E): 8d \times 5 μ M

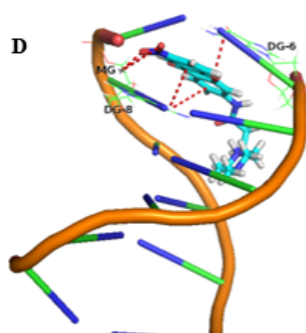
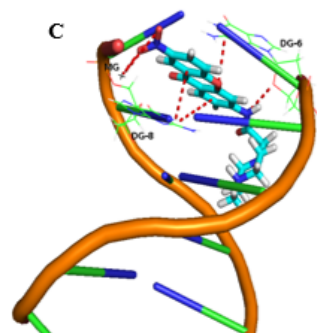
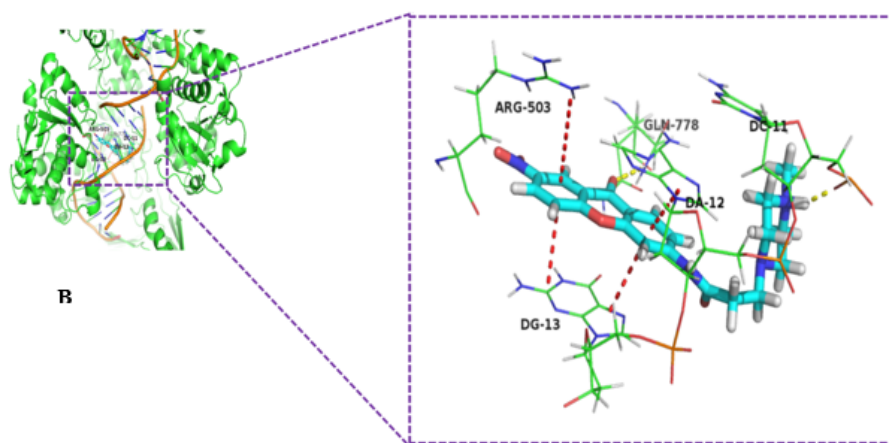
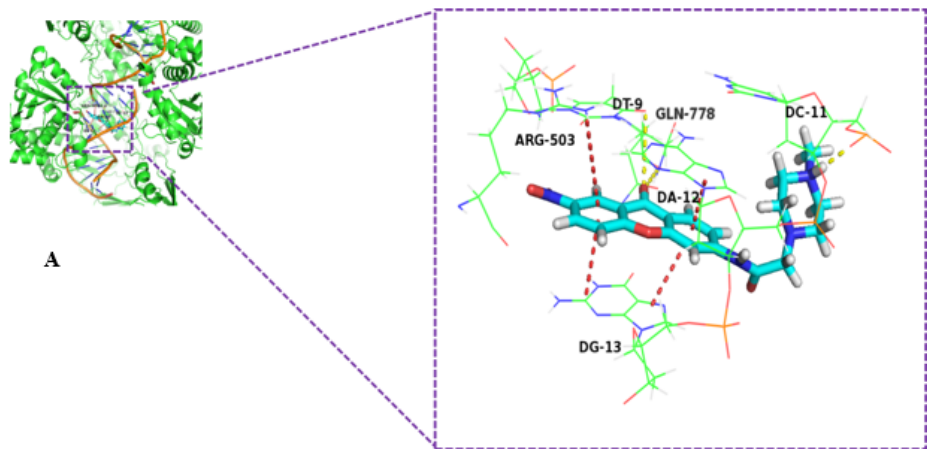


Figure 8

Docking pattern of compounds 7d (A) and 8d (B) with DNA topoisomerase II (PDB ID: 4G0V); Binding pose of compounds 7d (C) and 8d (D) with DNA (PDB ID: 2DES)

Supplementary Files

This is a list of supplementary files associated with this preprint. Click to download.

- [GraphicalAbstract.png](#)
- [Scheme1.png](#)
- [SupportingInformation.docx](#)